CHARACTERIZATION OF TUNNELING MAGNETO RESISTIVE HEADWITH MULTI-STRIPE HEIGHT BY USING FERRO MAGNETIC RESONANCE ANALYZER

PRAPINPORN WEAWHONGSE

A THESIS SUBMITTED IN PARTIAL FULFILLMENT
OF THE REQUIREMENT FOR THE DEGREE OF
MASTER OF ENGINEERING IN DATA STORAGE TECHNOLOGY
INTERNATIONAL COLLEGE
KING MONGKUT'S INSTITUTE OF TECHNOLOGY LADKRABANG
2014

KMITL-2014-IC-M-005-004

CHARACTERIZATION OF TUNNELING MAGNETO RESISTIVE HEAD WITH MULTI-STRIPE HEIGHT BY USING FERRO MAGNETIC RESONANCE ANALYZER

PRAPINPORN WEAWHONGSE

A THESIS SUBMITTED IN PARTIAL FULFILLMENT
OF THE REQUIREMENT FOR THE DEGREE OF
MASTER OF ENGINEERING IN DATA STORAGE TECHNOLOGY
INTERNATIONAL COLLEGE
KING MONGKUT'S INSTITUTE OF TECHNOLOGY LADKRABANG
2014

KMITL-2014-IC-M-005-004

Thesis	Characterization of Tunneling Magneto Resistive Head with Multi-Stripe Height by Using Ferromagnetic Resonance Analyzer
Student	Miss Prapinporn Weawhongse
Student ID.	53600604
Degree	Master of Engineering
Program	Data Storage Technology
Year	2014
Thesis Advisor	Asst.Prof.Dr.Kasin Vichienchom
Thesis Co-Advisor	Asst.Prof.Dr.Chiranut Sa-ngiamsak
Thesis Co-Advisor	Assoc.Prof.Dr.Wanchai Pijitrojana

ABSTRACT

The optimization of Stripe Heights (SH) scale of magnetic read sensor is conventionally determined by using quasi-static testing (QST) which provide electrical properties of the reader; however, the failures of magnetic read sensor are composed of hard and soft failure. QST can detect only on hard failure phenomena and some part of soft failure. Ferromagnetic resonance analyzer (FMRA) is additionally applied to optimize SH in finer scale by taken the magnetic property into consideration. The final outcome of this work can reduce the number of weak magnetic read sensors which might have malfunction of magnetic properties at early state and hence the cost of manufacturing. There were three conditions of the experiment composed of no external magnetic field, applying external magnetic field in longitudinal direction and applying transverse field in opposite polarities to study the behavior of magnetic read sensor by layer-level state. All the experiments were conducted with two levels of biasing voltages in forward and reverse directions in order to investigate the effect of heat and also the switching time of the magnetic read sensor in both directions. It is found that the SH scale plays some roles on the effective stiffness field of free layer due to change of shape anisotropy. The result has shown increased effective stiffness field as the SH is shorter which it can be observed through the trend of increasing in FMR frequency and decreasing in FMR amplitude. QST result has corresponded to the effective stiffness field trend which has presented less sensitivity and lower signal to noise ratio at the shorter SH. Once the high external magnetic field has been applied in longitudinal direction, FMR spectrums have been slightly changed on various SH scales caused by external magnetic field driven the magnetization of free layer into the saturation state while

for the longer SH a secondary FMR peak in high frequency has been found. The detailed analysis seems that this additional FMR peak has been the result of weaken magnetization of permanent magnet. In term of symmetrical characteristic of magnetic read sensor, the study suggest that overlapping has been better than underlapping because it is more symmetry at the shorter SH. FMR data can provide the finer limitation of SH for lapping process in a narrower range than that of QST. The SH limit by FMRA has shown that it should not be over +10nm from nominal while QST data has indicated the limit at +20nm from nominal. These results imply that FMR data is able to identify the finer scale of SH for lapping process. The cost reduction is gained for less drive failure by providing information for lapping process with finer range of lapping.

Acknowledgement

First of all, I would like to express my sincere gratitude to Asst.Prof.Dr.Kasin Vichienchom (King Mongkut's Institute of Technology Ladkrabang), Asst.Prof.Dr.Chiranut Sa-ngiamsak (Khon Kaen University) and Assoc.Prof.Dr.Wanchai Pijitrojana (Thammsat University) for guidance, advice and review of my work.

I wish to express my gratitude to Western Digital (Thailand) Co., Ltd. for granting the scholarship at the International College, King Mongkut's Institute of Technology Ladkrabang. Also I appreciate the Design Optimization Engineering team at Western Digital (Thailand) that kindly supported the FMR laboratory to conduct the thesis work and provide useful information for this study. I also express my sincere thanks and gratitude to my supervisors from the Product Engineering team at Western Digital (Thailand) for supporting my master study and also thank my colleagues for the valuable comments and recommendations. Furthermore, I would like to thank all the KMITL friends for the pleasant and encouraging atmosphere during our master study.

Finally, I am really grateful to my family for their motivation and support throughout my life.

Prapinporn Weawhongse

Contents

Page

Abstract.....I

Acknowledgement.....III

Contents.....IV

List of Tables.....VI

List of Figures.....VII

Chapter 1 Introduction.....1

1.1 Statement of problem.....1

1.2 Objectives.....2

1.3 Scope and limitations.....3

1.4 The conceptual framework.....4

Chapter 2 Theory and Literature Review.....5

2.1 Introduction.....5

2.2 Principle of Tunneling Magneto Resistive (TMR).....5

2.3 Magnetic read sensor configuration.....10

2.4 Standard characterization tool.....13

2.5 Advanced characterization tool.....16

Chapter 3 Methodology and Experiment.....21

3.1 Introduction 21

3.2 Manufacturing process of magnetic sensor.....21

3.3 Sample specifications.....22

3.4 Characterization tools.....22

3.5 Flow chart of the experiment.....24

Contents (Cont.)

Page

Chapter 4 Experimental Results....26

4.1 Introduction....26

4.2 FMR spectrum as function of no external magnetic field....26

4.3 Longitudinal field dependence of the FMR spectrum....37

4.4 Transverse field dependence of the FMR spectrum....47

Chapter 5 Conclusions and Suggestions....52

Reference....54

Appendices....56

List of Tables

Tables Page
3.1 The experimental set up.....25
4.1 Summary of the FMR result for magnetic read sensor with seven SH targets from -20nm SH to +20nm SH target without applying external magnetic field.....27
4.2 Summary of the QST result between -20nm SH to +20nm SH target.....31
4.3 Summary of the FMR result for magnetic read sensor with seven SH targets from -20nm SH to +20nm SH target with +1.2 kOe applying external magnetic field.....39
4.4 Summary of the FMR result for magnetic read sensor with seven SH targets from -20nm SH to +20nm SH target with -1.2 kOe applying external magnetic field.....44
4.5 Summary of the delta FMR between with +520Oe and -520 Oe applying external magnetic field in transverse direction for magnetic read sensor with seven SH targets from -20nm SH to +20nm SH target.....50

List of Figures

Figures Page
1.1 Revolution of reader technology.....1
1.2 Physical dimension of magnetic read sensor.....2
1.3 Conceptual framework.....4
2.1 FM/I/structure on TMR head.....5
2.2 Energy bands of a non-magnetic metal at the Fermi level. The down-spin and up-spin electrons are equal in the *d* band.....6
2.3 Energy bands in a FM/NM/FM structure. (a) The magnetizations of two ferromagnetic layers are parallel state. (b) The magnetizations of two ferromagnetic layers are anti-parallel state.....7
2.4 Electron transport in a FM/NM/FM structure. (a) The magnetizations of two ferromagnetic layers are parallel. The bottom picture shows the resistor network in two-channel mode. (b) The magnetizations of two ferromagnetic layers are antiparallel. The lower parts of diagram show the resistor network in two-channel mode.....8
2.5 Scaling estimate of read head dimension in terms of recorded bit (Gbit/in2), showing the sensor read width RW (red line) and shield-to-shield total gap spacing (blue line).....10
2.6 Thin film head structure as viewed from the media disk.....11
2.7 Simulation model of TMR read.....11
2.8 Simple diagram of free layer and pinned layer magnetization vectors.....12
2.9 QST transfer curve.....13
2.10 Definition of QST transfer curve.....14
2.11 MRR test.....14
2.12 The precession of the magnetization around the effective field according to the Landau-Lifshitz-Gilbert equation (LLG) 17
2.13 Ferro magnetic resonance (FMR) spectrum.....18
3.1 Manufacturing process of magnetic head sensor.....21
3.2 Flow of experiment process.....22
3.3 Ferromagnetic resonance test.....23
3.4 Flow chart of the experiment.....25
4.1 FMR spectrum without applying external magnetic field with +140 mV volt bias for two different SH targets of TMR sensor (a) shortest SH target is -20nm SH from nominal (b) longest SH target is +20nm SH from nominal.....27

List of Figures (Cont.)

Figures Page
4.2 FMR spectrum trend of magnetic read sensor with various SH targets without applying external magnetic field and varied set up of volt biases.....28
4.3 FMR spectrum without applying external magnetic field with +160 mV volt bias for two different SH targets of TMR sensor (a) shortest SH target is -20nm SH from nominal (b) longest SH target is +20nm SH from nominal.....29
4.4 FMR spectrum without applying external magnetic field with -140 mV volt bias for two different SH targets of TMR sensor (a) shortest SH target is -20nm SH from nominal (b) longest SH target is +20nm SH from nominal.....30
4.5 FMR spectrum without applying external magnetic field with -160 mV volt bias for two different SH targets of TMR sensor (a) shortest SH target is -20nm SH from nominal (b) longest SH target is +20nm SH from nominal.....30
4.6 Transfer curve of magnetic read sensor with +140 mV volt bias for two different SH targets of TMR sensor (a) shortest SH target is -20nm SH from nominal (b) longest SH target is +20nm SH from nominal 32
4.7 QST trend of magnetic read sensor with various SH scales from -20nm SH target to +20nm SH target.....33
4.8 Transfer curve of magnetic read sensor with +160 mV volt bias for two different SH targets of TMR sensor (a) shortest SH target is -20nm SH from nominal (b) longest SH target is +20nm SH from nominal 34
4.9 Transfer curve of magnetic read sensor with -140 mV volt bias for two different SH targets of TMR sensor (a) shortest SH target is -20nm SH from nominal (b) longest SH target is +20nm SH from nominal 34
4.10 Transfer curve of magnetic read sensor with -160 mV volt bias for two different SH targets of TMR sensor (a) shortest SH target is -20nm SH from nominal (b) longest SH target is +20nm SH from nominal 34
4.11 Correlation between FMR frequency and MRR at QST 35
4.12 Correlation between FMR frequency and Amplitude at QST.....36
4.13 Correlation between FMR frequency and SNR at QST.....36
4.14 FMR spectrum with applying +1.2 kOe external magnetic field with +140 mV volt bias for two different SH targets of TMR sensor (a) shortest SH is -20nm SH from nominal (b) longest SH is +20nm SH from nominal.....37

List of Figures (Cont.)

Figures Page
4.15 FMR spectrum with applying +1.2 kOe external magnetic field with -140 mV volt bias for two different SH targets of TMR sensor (a) shortest SH target is -20nm SH from nominal (b) longest SH is +20nm SH from nominal.....38
4.16 FMR spectrum with applying +1.2 kOe external magnetic field with +160 mV volt bias for two different SH targets of TMR sensor (a) shortest SH target is -20nm SH from nominal (b) longest SH target is +20nm SH from nominal.....38
4.17 FMR spectrum with applying +1.2 kOe external magnetic field with -160 mV volt bias for two different SH targets of TMR sensor (a) shortest SH target is -20nm SH from nominal (b) longest SH target is +20nm SH from nominal.....38
4.18 FMR spectrum trend of magnetic read sensor with various SH targets with +1.2 kOe applying external magnetic field 40
4.19 FMR spectrum with applying -1.2 kOe external magnetic field with +140 mV volt bias for two different SH targets of TMR sensor (a) shortest SH target is -20nm SH from nominal (b) longest SH target is +20nm SH from nominal.....42
4.20 FMR spectrum with applying -1.2 kOe external magnetic field with -140 mV volt bias for two different SH targets of TMR sensor (a) shortest SH target is -20nm SH from nominal (b) longest SH target is +20nm SH from nominal.....43
4.21 FMR spectrum with applying -1.2 kOe external magnetic field with +160 mV volt bias for two different SH targets of TMR sensor (a) shortest SH target is -20nm SH from nominal (b) longest SH target is +20nm SH from nominal.....43
4.22 FMR spectrum with applying -1.2 kOe external magnetic field with -160 mV volt bias for two different SH targets of TMR sensor (a) shortest SH target is -20nm SH from nominal (b) longest SH target is +20nm SH from nominal 43
4.23 FMR spectrum trend of magnetic read sensor with various SH targets with -1.2 kOe applying external magnetic field.....45
4.24 Overall FMR spectrum trend with applying external magnetic field in longitudinal direction on magnetic read sensor with various SH targets 46
4.25 FMR spectrum with applying +520 Oe and -520 Oe transverse field with +140 mV volt bias for two SH targets of TMR sensor (a) shortest SH target is -20nm SH from nominal (b) longest SH target is +20nm SH from nominal.....48

List of Figures (Cont.)

Figures Page
4.26 FMR spectrum with applying +520 Oe and -520 Oe transverse field with -140 mV volt bias for two SH targets of TMR sensor (a) shortest SH target is -20nm SH from nominal (b) longest SH target is +20nm SH from nominal.....49
4.27 FMR spectrum with applying +520 Oe and -520 Oe transverse field with +160 mV volt bias for two SH targets of TMR sensor (a) shortest SH target is -20nm SH from nominal (b) longest SH target is +20nm SH from nominal.....49
4.28 FMR spectrum with applying +520 Oe and -520 Oe transverse field with -160 mV volt bias for two SH targets of TMR sensor (a) shortest SH target is -20nm SH from nominal (b) longest SH target is +20nm SH from nominal.....49
4.29 The trend of delta FMR spectrum with applying opposite polarity transverse field (+520 Oe and -520 Oe) on magnetic read sensor with various SH targets.....51

Chapter 1
Introduction

1.1 Statement of Problem

According to continued increase of areal density in magnetic recording [1], the dimension of magnetic read and write sensor are continued decreasing with complex designs. Presently, magnetic read sensor is based on Tunneling Magneto Resistance (TMR) technology as shown in Fig. 1.1, which is able to improve the read ability and reliability as shrinking size.

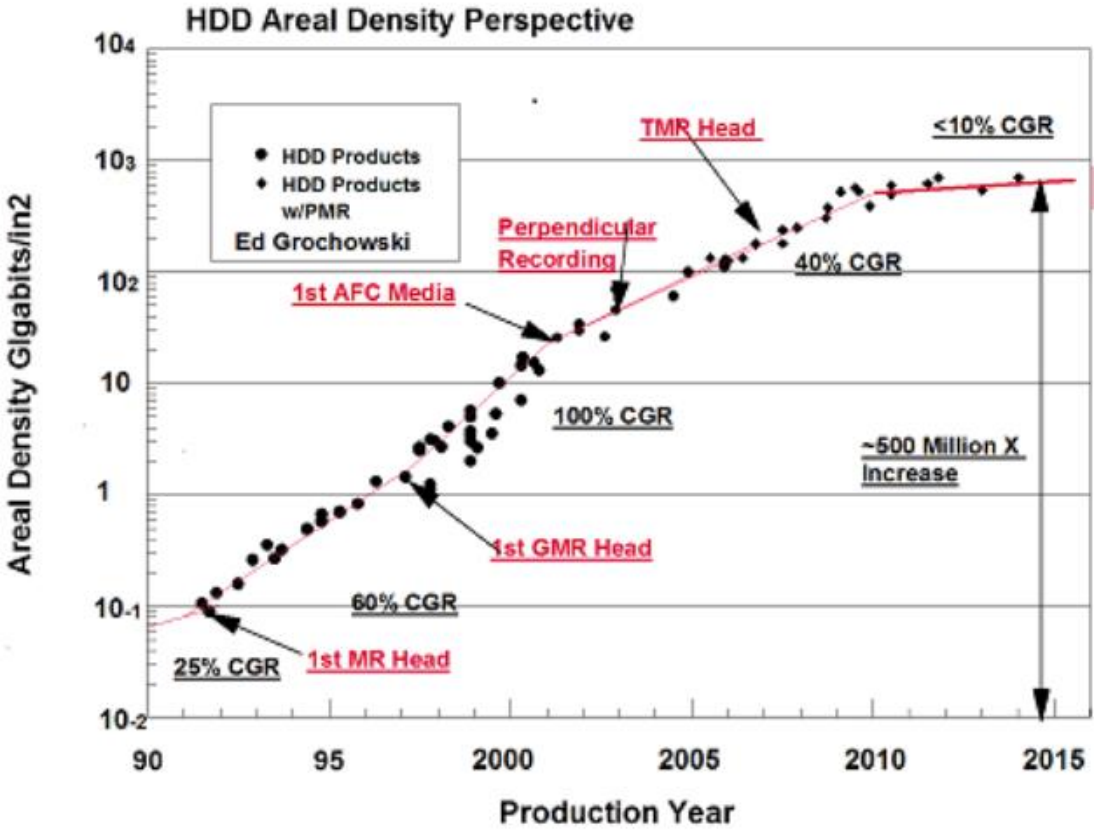

Fig. 1.1 Revolution of reader technology [1]

Stripe Height (SH) is a key physical dimension which is a length of magnetic read sensor [2] as shown in Fig. 1.2. It is controlled by lapping process of slider fabrication. The SH is proportional to the volume of magnetic read sensor that significantly impacts to head sensitivity. As continued reducing track width (TW) of magnetic read sensor to gain areal density, SH is needed to scale down to keep aspect ratio (TW/SH) which is for maintaining resistance and signal constant of read sensor.

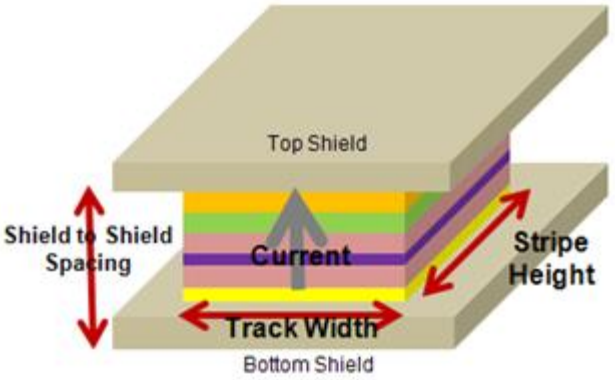

Fig. 1.2 Physical dimension of magnetic read sensor [2]

The optimization of SH scale of magnetic read sensor is conventionally determined by using quasi-static testing (QST). QST is used to get the response of magnetic read sensor in applied external magnetic field by sweeping from negative to positive field without flying head over the media, and then the transfer curve and noise of magnetic recording are obtained. This tool provides electrical properties of the reader; however, the failures of magnetic read sensor are composed of hard and soft failure. QST can detect only on hard failure phenomena and some part of soft failure [3]. Ferromagnetic resonance analyzer (FMRA) [4] is additionally applied to optimize the SH in finer scale by taken the magnetic property into consideration. To extend the study, this paper is proposed to further characterize the magnetic read sensor with various SH scales by using FMRA. FMRA is an equipment to perform magnetic properties that are related to magnetization fluctuation in different layers of read head sensor. FMRA is able to explain the behavior of magnetic reader sensor by layer-level state in term of stiffness field which is related to efficiency of read sensor. Therefore, we can understand the source of magnetic read sensor behavior and apply to extend the detection capabilities for magnetic recording industry. The final outcome of this work can reduce the number of weak magnetic read sensors which might have malfunction of magnetic properties at early state and hence the cost of manufacturing.

1.2 Objectives

The objective of this research is to study the behavior of TMR sensor with multi-stripe height by using ferromagnetic resonance analyzer (FMRA) in comparison to quasi-static test (QST).

1.3 Scope and limitations

This study has scope and limitation as following.

1.3.1 The experiment is characterized on TMR sensor with the same areal density and TW with seven SH targets.

1.3.2 FMRA is used to study the magnetic properties of read sensor by layer-level state in the range of 0.3-10 GHz. The FMRA parameters focused in the experiment are shown as below:

1.3.2.1 FMR peak frequency

1.3.2.2 FMR peak amplitude

1.3.2.3 FMR peak resonance width

1.3.2.4 FMR secondary peak

1.3.3 QST is applied to measure the electrical properties of read sensor while applying the external magnetic field. The QST parameters focused in the experiment are shown as below:

1.3.3.1 Amplitude

1.3.3.2 Signal to Noise ratio (SNR)

1.3.3.3 Magneto-Resistance Resistivity (MRR)

1.3.3.4 Asymmetry

1.3.3.5 Barkhausen Jump

1.3.3.6 Hysteresis

1.3.4 Magnetic read sensor is performed in bar level as FMR measurement is able to test on bar form.

1.3.5 The experiment is focused on magnetic read sensor; as a result there is no dynamic electrical test which is related writer sensor.

1.4 The conceptual framework is shown in Fig. 1.3.

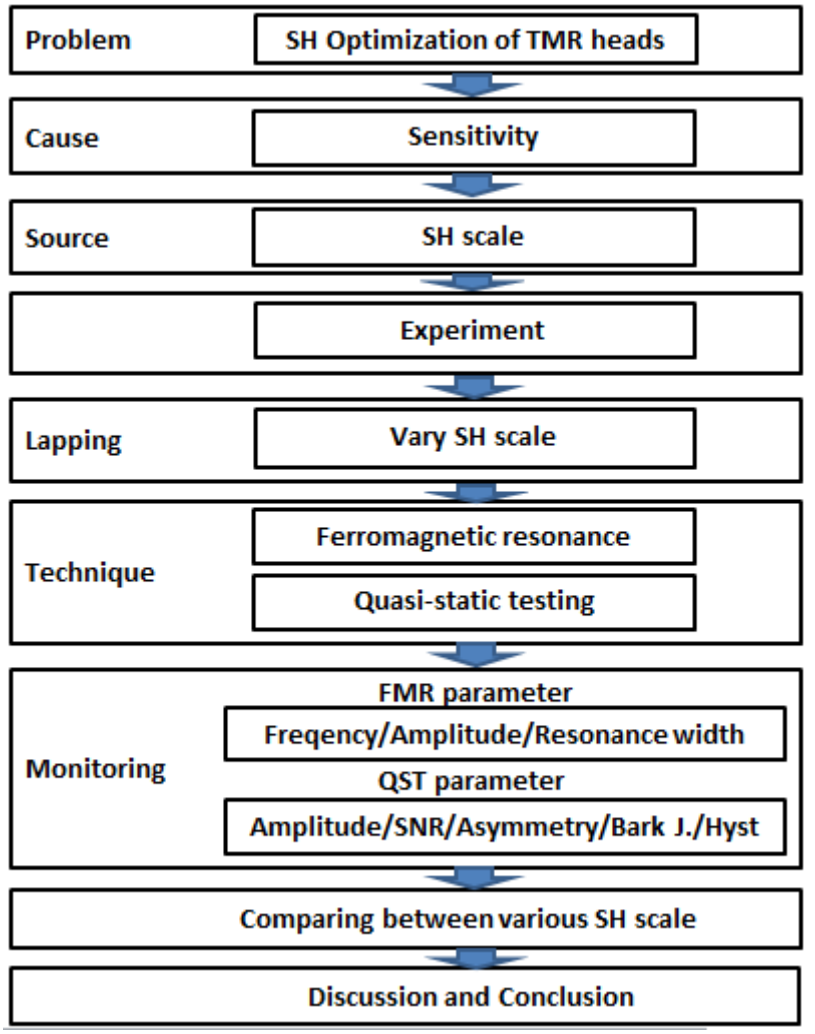

Fig. 1.3 Conceptual framework

Chapter 2
Theory and Literature Review

2.1 Introduction

Tunneling magneto resistive (TMR) head has been widely used in high-density magnetic recording to read back signal that is recorded in magnetic media [5]-[7]. The magnetic read sensors keep shrinking the dimension with complex design to support increased areal density requirement. It is very important to understand the TMR head characteristic in order to enhance the read ability of magnetic read sensor. Therefore, the first part of this chapter describes a principle and component of TMR head technology. Second part is characteristic tools for magnetic read sensor in industry that are composed of standard and advanced tool. The standard tool is quasi-static test (QST) and advanced tool is ferromagnetic resonance analyzer (FMRA). The last part is ferromagnetic resonance theory that is the proposed technique to carry on the experiment.

2.2 Principle of Tunneling Magneto Resistive (TMR)

Tunneling magnetoresistance (TMR) is due to phenomenon of spin-polarized tunneling [8]. TMR consists of ferromagnetic layers to form thin film that is separated by thin insulating barrier as shown in Fig. 2.1 [8]. In 1975, Julliere proposed the predicted model of tunneling magnetoresistance. The experiment was done on two ferromagnetic electrodes which were Co and Fe that were separated by Ge thin insulating. The experiment showed that the resistance depended on magnetization direction of Co and Fe that was aligned in parallel or anti-parallel direction.

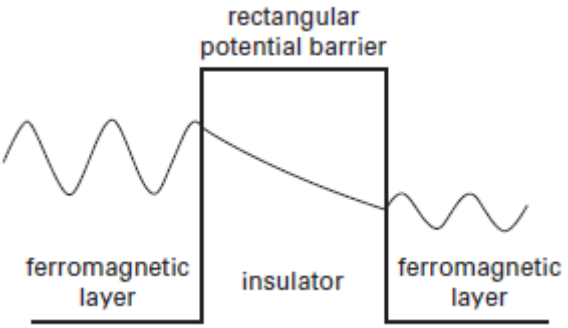

Fig. 2.1 FM/I/FM structure on TMR head [8]

Therefore, the tunnel resistance depends on the relative orientation of the magnetization on both sides of the barrier. The tunneling magnetoresistance (TMR) ratio is given by [8]

$$TMR = \frac{\Delta R}{R_p} = \frac{R_{ap} - R_p}{R_p} = \frac{2P_1P_2}{1 - P_1P_2} \tag{2.1}$$

where R_{ap} and R_p are the resistances when the magnetizations of the ferromagnetic layers are antiparallel and parallel, respectively.

The magneto resistance effect can be studied as the following detail. The electrical conductivity in metals is described by considering two conductivity channels which corresponds to the up-spin and down-spin electrons. The difference in scattering between the antiparallel and parallel alignment multilayers is explained by using a band structure picture as shown in Fig. 2.2 [8]. In normal metal there are equal numbers of up-spin and down-spin states at the Fermi level. As a result, up and down-spin electrons are travelled through a normal metal with equal probability.

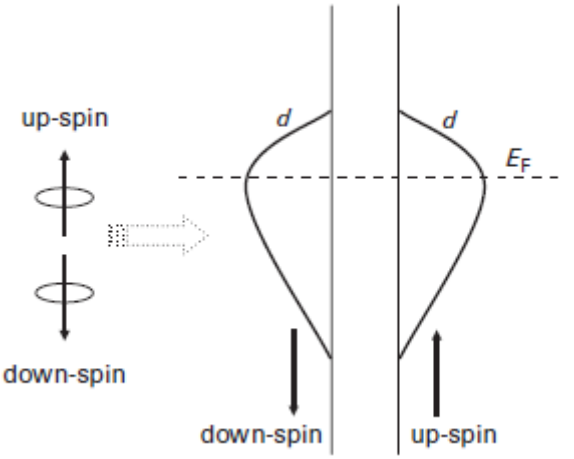

Fig. 2.2 Energy bands of a non-magnetic metal at the Fermi level. The down-spin and up-spin electrons are equal in the *d* band [8]

In a spin-polarized metal, there are more stated of one spin direction than the other at the Fermi level as depicted in Fig. 2.3 [8]. The density of states at the Fermi level is different between up-spin and down-spin. Generally, the majority-spin electrons in which the spin of the electrons is parallel to the direction of magnetization of the ferromagnet have a weak scattering as shown in Fig. 2.3 (a). Moreover, the minority-spin electrons in which the spin of the electrons is antiparallel to the direction of magnetizations of ferro-magnet have a strong scattering. Hence, there are the different resistances of two spin electrons.

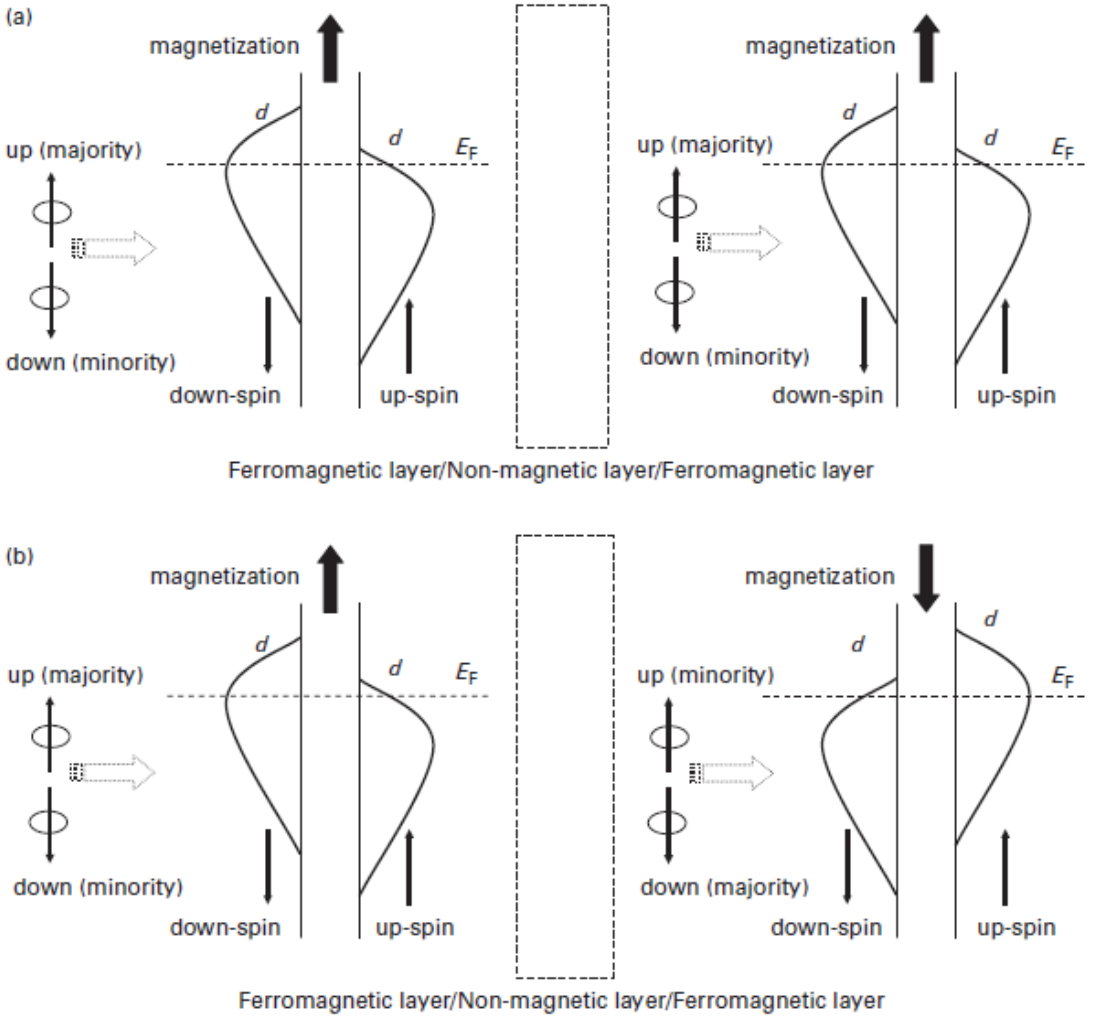

Fig. 2.3 Energy bands in a FM/NM/FM structure. (a) The magnetizations of two ferromagnetic layers are parallel state. (b) The magnetizations of two ferromagnetic layers are anti-parallel state [8]

Figure 2.4 [8] presents the electron transport in magnetic multilayers which is similar to Fig. 2.3 but they are composed of resistor network in two-channel mode at the bottom part. In Fig. 2.4 (a), the up-spin electrons are weakly scattered and the down-spin electrons are strongly sacttered in both ferrromagnetic layers. The resistance is modeled by two small resistance $R_{\uparrow}$ in the up-spin channel and by two large resistances $R_{\downarrow}$ in the down-spin channel. While the condition of the antiferrromagnetically aligned multilayer as shown in Fig. 2.4 (b), the up-spin electrons are weakly scattered in the bottom ferromagnetic layer and are strongly scattered in the top ferromagnetic layer. The down-spin electrons are strongly scattered in the bottom ferrromagnetic layer and are weakly scattered in the top ferrromagnetic layer.

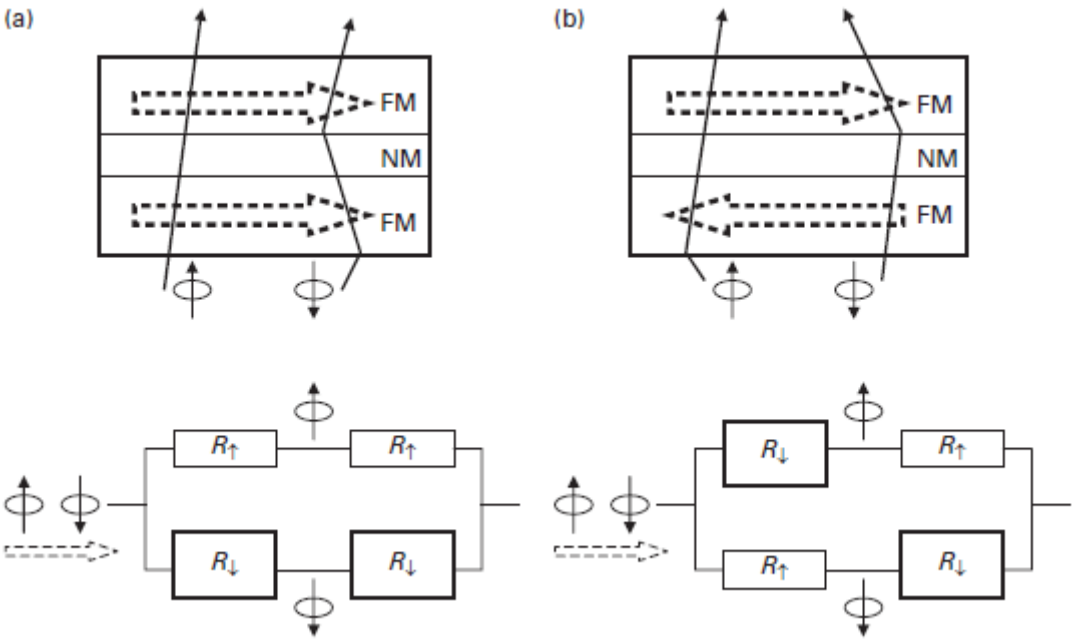

Fig. 2.4 Electron transport in a FM/NM/FM structure. (a) The magnetizations of two ferromagnetic layers are parallel. The bottom parts show the resistor network in two-channel mode. (b) The magnetizations of two ferromagnetic layers are antiparallel. The bottom parts of diagram present the resistor network in two-channel mode [8]

If the up-spin and down-spin resistor channels are connected in parallel, the total resistance $\left(R_p\right)$ which is shown in Fig. 2.4 (a) can be calculated by [8]

$$R_p = \frac{1}{\frac{1}{2R_\uparrow} + \frac{1}{2R_\downarrow}} = \frac{2R_\uparrow R_\downarrow}{R_\uparrow + R_\downarrow} \tag{2.2}$$

At the magnetizations of two ferromagnetic layers are antiparallel, the total resistance can be described as $\left(R_{ap}\right)$ follows [8]

$$R_{ap} = \frac{R_\uparrow + R_\downarrow}{2} \tag{2.3}$$

Hence, the different resistance between two cases is given by [8]

$$\Delta R = R_p - R_{ap} = -\frac{1}{2}\frac{\left(R_\uparrow - R_\downarrow\right)^2}{R_\uparrow + R_\downarrow} \tag{2.4}$$

From Equation 2.4, we observe that the larger the difference between $R_{\uparrow}$ and $R_{\downarrow}$, which are displayed the larger the magnetoresistance. According to Julliere's proposed, TMR depends on spin polarization that is given by [8]

$$TMR = \frac{2P_1P_2}{1-P_1P_2} \tag{2.5}$$

Where P_1 and P_2 are the spin polarization of two ferromagnetic layers. The spin polarized electron in the ferromagnetic is explained as follows [8]

$$P_i = \frac{D_{i\uparrow} - D_{i\downarrow}}{D_{i\uparrow} + D_{i\downarrow}} \tag{2.6}$$

Where $D_{1\uparrow(\downarrow)}$ and $D_{2\uparrow(\downarrow)}$ are the DOS of two ferromagnetic electrode at the Fermi level for the two spin directions.

In 1989, Slonczewski proposed a theory to analyze the transmission of spin-polarized electrons travelling through a tunneling barrier. The theory is based on the free-electron model, and the *Schrödinger* equation is solved to find out the conductance as a function of the relative magnetization alignment of the two ferromagnetic layers. The conductance dependence on the angle θ between the magnetizations of the two ferromagnetic layers is presented as follows [8]

$$G(\theta) = G_s\left(1 + P_F^2 \cos\theta\right) \tag{2.7}$$

where G_s is the mean surface conductance and is independent of θ, and P_F is the effective spin polarization of the tunneling electrons given by [8]

$$P_F = \frac{k^{\uparrow} - k^{\downarrow}\kappa^2 - k^{\uparrow}k^{\downarrow}}{k^{\uparrow} + k^{\downarrow}\kappa^2 + k^{\uparrow}k^{\downarrow}} \tag{2.8}$$

Where $k^{\uparrow}$ is the Fermi wave vector in the up-spin band, $k^{\downarrow}$ is the Fermi wave vector in the down-spin band and $i\kappa$ is the imaginary wave vector in the barrier. Note that is determined by the potential barrier V_b [8]

$$\kappa = \frac{1}{\bar{h}}\sqrt{2m\left(V_b - E_F\right)} \tag{2.9}$$

The E_F is the Fermi energy. In the limit of a high potential barrier, κ approaches ∞.Therefore, the spin polarization from Equation (P_F) are turned as follows [8]

$$\lim_{\kappa\to\infty} P_F = \frac{k^{\uparrow} - k^{\downarrow}}{k^{\uparrow} + k^{\downarrow}} \tag{2.10}$$

2.3 Magnetic read sensor configuration

As continued increase of areal density in magnetic recording, the dimension of magnetic read senor is continued decreasing with complex designs as shown in Fig. 2.5 [9]. Presently, magnetic read sensor is based on TMR technology that is high sensitivity, large signal to noise ratio and stable recording head for digital information processing.

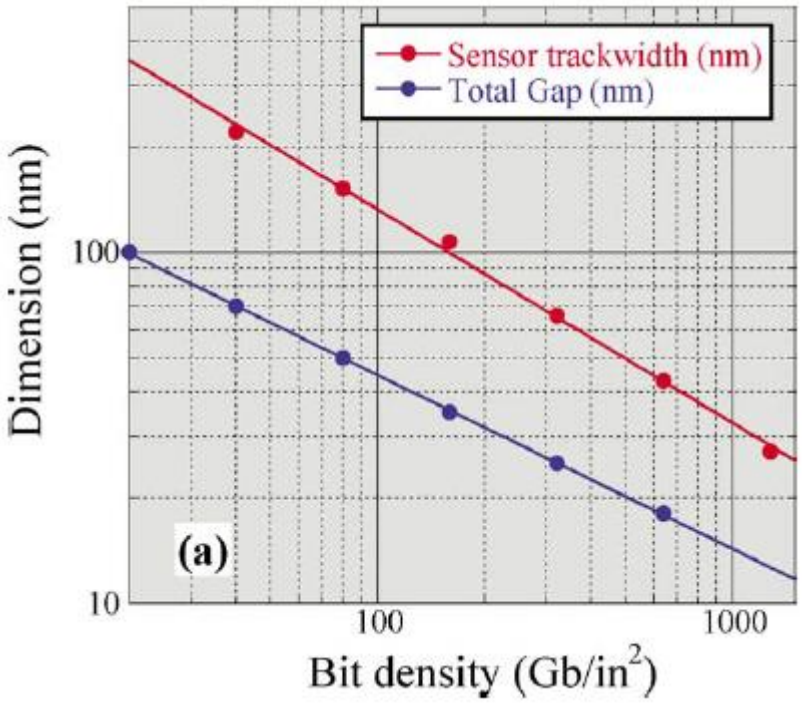

Fig. 2.5 Scaling estimate of read head dimension in terms of recorded bit (Gbit/in2), showing the sensor read width RW (red line) and shield-to-shield total gap spacing (blue line) [9]

Figure 2.6 shows the magnetic read head structure which is located between two shields as viewed from the media disk surface [9]. TMR reader head consists of multiple magnetic thin films as illustrated in Fig. 2.7 [10]. The major components of multilayer thin films have free magnetic layer, tunnel barrier, pinned layer, pinning layer and hard bias which have more detail as following.

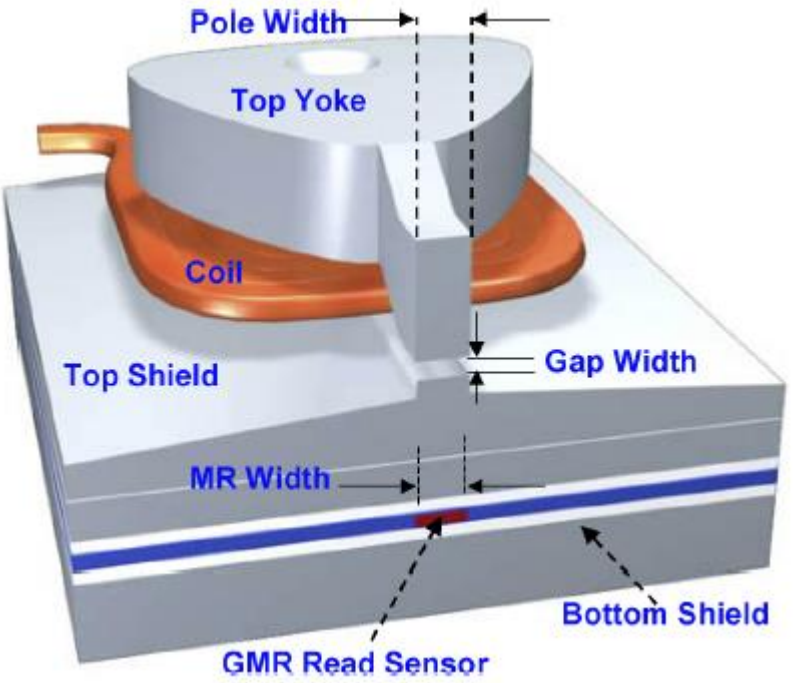

Fig. 2.6 Thin film head structure as viewed from the media disk [9]

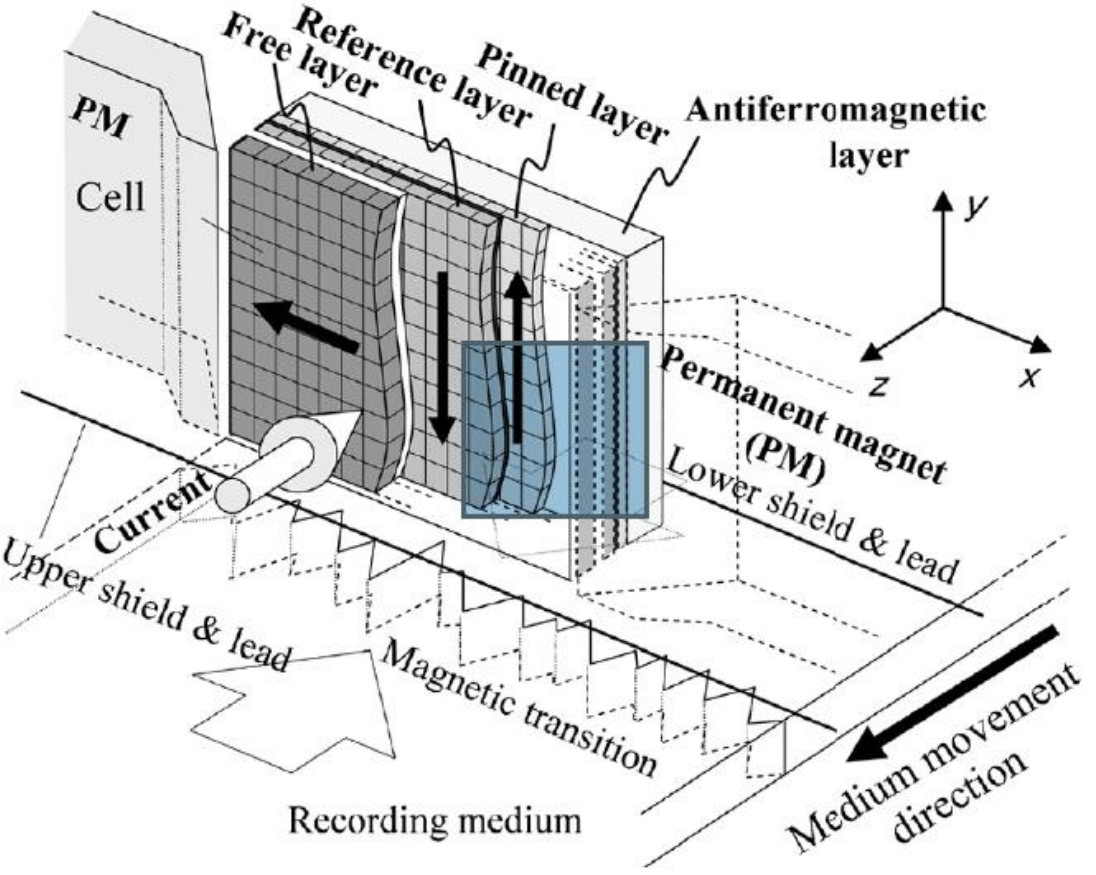

Fig. 2.7 Simulation model of TMR read [10]

2.3.1 Free layer is made of ferromagnetic material and magnetization in this layer can be rotated and used to sense a magnetic field from media. This layer can be called “sensing layer”

2.3.2 Tunnel barrier layer is made of non-magnetic a material that is insulator.

2.3.3 The Reference and pinned layer is made of ferromagnetic material that sandwich by Ru layer. The magnetization direction is fixed (pinned) by the AFM (Anti Ferromagnetic) layer.

2.3.4 AFM (Anti ferromagnetic) layer normally behaves as a non-magnetic material. But can pin magnetization of the pinned layer that is called “Exchange bias”

2.3.5 Permanent magnet (PM) is to stabilize the free layer. It is polycrystalline in nature with the magnetic coerciveness that originate from magneto crystalline anisotropy.

Magnetic media generates magnetic fields that intercept to the magnetic read sensor which causes the change of magnetization direction of the free layer.This magnetic orientation can be achieved by means of the permanent magnets which give the biasing field to the free layer. Then magnetization alignments between the pinned and the free layers become either parallel or anti-parallel direction contributing to have low or high resistance. A large change in resistance that result to high TMR ratio can be measured and explained by the principle of magneto resistance as previous detail. Figure 2.8 shows a simple diagram of magnetic read sensor which is composed of free layer and pinned layer magnetization vectors [11].

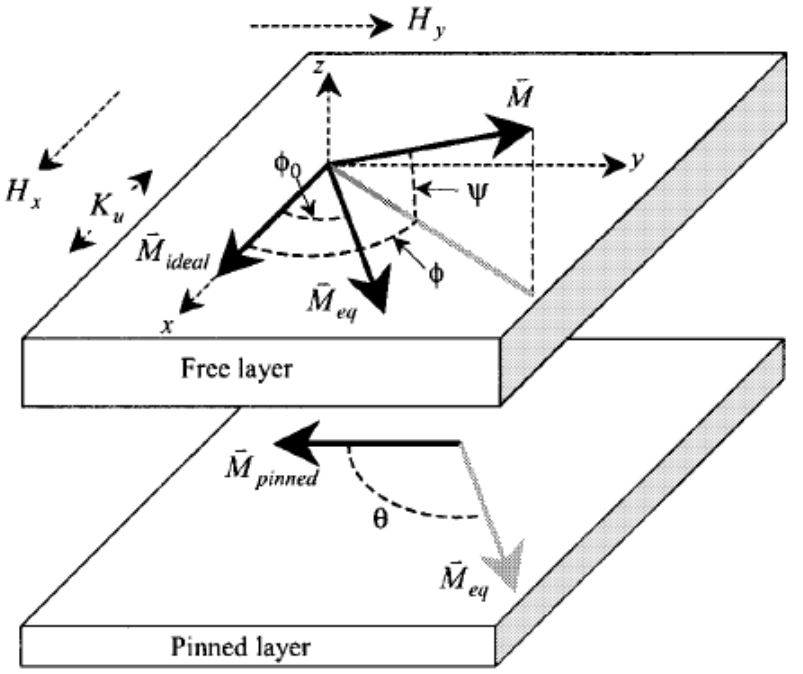

Fig. 2.8 Simple diagram of free layer and pinned layer magnetization vectors [11]

Free layer magnetization (top), at equilibrium $\vec{M}_{eq}$ makes an angle θ with respect to the pinned layer magnetization (bottom). For best sensitivity, $\theta = \pi/2$; the magnetization in this ideal position is indicated by $\vec{M}_{ideal}$ which the magnetization orientation of free layer is aligned perpendicular to pinned layer [11]. The longitudinal field H_x is from permanent magnetic hard bias and transvers field H_y is due to bias current which are shown in Fig. 2.8. The crystalline anisotropy energy is K_u ; the crystalline anisotropy axis is parallel to H_x. Because of the transverse field, $\vec{M}_{eq}$ is not aligned with $\vec{M}_{ideal}$; the angle between them is ϕ_0. The instantaneous magnetization $\vec{M}$ is fluctuating quantity which makes an angle to the xy plane ϕ with the anisotropy axis. The magnetization also tilts out of the xy plane by an angle ψ. As we have discussed about ideal condition, magnetic read sensor gains best sensitivity and symmetry sensor response [4]. Nevertheless, the magnetization tilt is possible to occur as decreasing the dimension of magnetic read sensor to support areal density which affects to sensitivity and instability problem.

2.4 Standard characterization tool

Quasi Static Test (QST) is a normal technique in the measurement of electrical properties of magnetic read sensor in hard disk drive (HDD) industry. It is the production test which runs after finishing slider fabrication process. QST is a static test that performs without flying head over a media to characterize whole the performance of magnetic read sensor. This tool measures the intrinsic magnetic read sensor response with applying external magnetic field in transverse direction by sweeping field from negative to positive field after that a transfer curve is obtained as shown in Fig. 2.9.

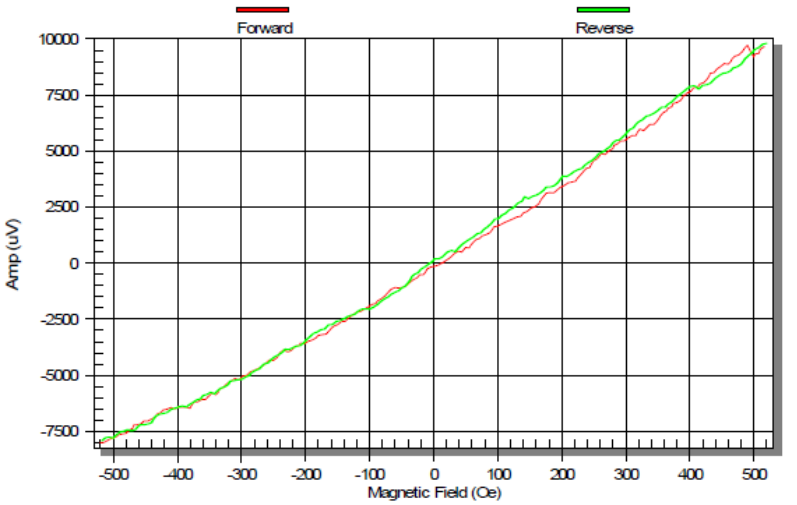

Fig. 2.9 QST transfer curve [2]

QST transfer curve provides the performance of magnetic read sensor such as sensitivity, noise and instability parameter. There are key parameters for characterizing the magnetic read sensor composed of Magneto-Resistive Resistance (MRR), Amplitude, Asymmetry, SNR and instability parameters. The Fig. 2.10 presents the definition of key QST parameters that are described as following detail [12].

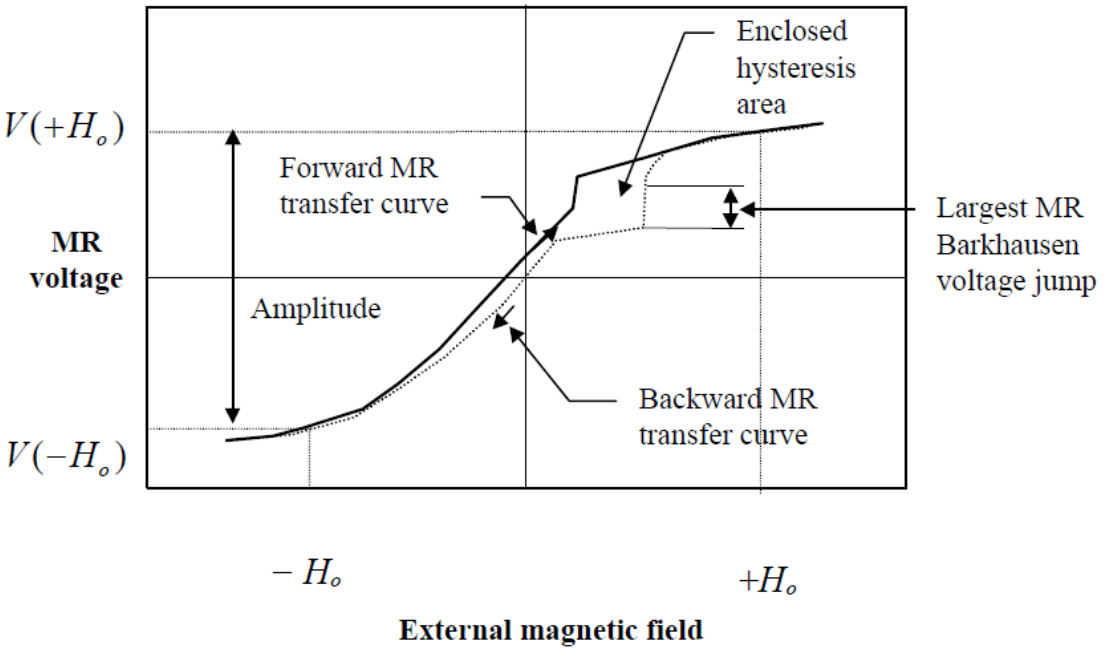

Fig. 2.10 Definition of QST transfer curve [12]

2.4.1 Resistance is measured the resistance of magnetic read head element by apply bias current pass through the read head with no magnetic field. The voltage is measured across read head as shown in Fig. 2.11.

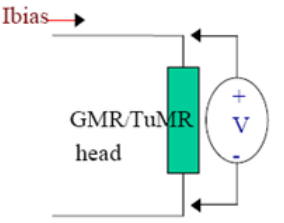

Fig. 2.11 MRR test [12]

Resistance is given by the following equation

$$R_{MR} = \frac{V_{MR}}{I_{Bias}} \tag{2.11}$$

2.4.2 Amplitude is composed of two types that are Amplitude at test and peak to peak Amplitude.

1. Amplitude at test (μV) is a peak Amplitude at the point that user is defined field location. This parameter is based on average value of the forward and reverse curves.

2. Peak to Peak Amplitude (μV) is calculated by the following equation

$$Pk-Pk\ \ Amp(\mu V)=Max\ \ Amp(\mu V)-Min\ \ Amp(\mu V) \tag{2.12}$$

2.4.3 Asymmetry is the relative difference between positive and negative signals that result from driven magnetic read head into saturation with no long linear response of the transfer curve as shown in Fig. 2.10. Asymmetry parameter also has two types as Amplitude such as Asymmetry at test and Peak to Peak Asymmetry as following.

1. Asymmetry at test (%) is to asymmetry that is calculated at user defined field location.

2. Peak to Peak Asymmetry (%) is calculated as follow

$$Asym=\frac{|Max|-|Min|}{|Max|+|Min|}\times 100 \tag{2.13}$$

2.4.4 Instability parameter is composed of Barkhausen Jump, hysteresis and signal to noise ratio (SNR) as follow

1. Barkhausen Jump is the maximum amplitude jump between two adjacent samples as shown in Fig. 2.10. This barkhausen effect is caused by rapid changed size of magnetic domains.

The relative value of Barkhausen jump can be calculated by below formula

$$Barkhausen\ Jump(\%)=\frac{Barkhausen\ Jump(\mu V)}{Pk-Pk\ \ Amp(\mu V)}\times 100 \tag{2.14}$$

Where Barkhausen Jump (μV) is the absolute value of the Barkhausen jump.

2. Hysteresis is the measurement area between forward and reverse curves as shown in Fig. 2.10. The Hysteresis is calculated by following formula

$$Hyst(\mu V/Oe)=Inc*\sum|Fi-Ri| \tag{2.15}$$

Where
Inc is field increment,
Fi is Amplitude at each i of forward curve
Ri is Amplitude at each i of reverse curve

$$Hysteresis(\%) = \frac{A}{B} * 100 \tag{2.16}$$

Where

A is Hysteresis as defined above

$$B = Inc \sum \frac{(Max_i + Min_i)}{2} - Min_i \tag{2.17}$$

3. Signal to noise ratio (SNR) is key focus for magnetic read head that is calculated by amplitude divided by noise. This SNR is tested under static level but still need high SNR as dynamic level.

QST is used for explaining the electrical properties and indicate the optimized SH of magnetic read sensor. However, QST data can detect only on hard failure phenomena and some part of soft failure. Ferromagnetic resonance analyzer (FMRA) is additionally applied to optimize SH in finer scale by taken the magnetic property into consideration that is described in the following part.

2.5 Advanced characterization tool

Ferro magnetic resonance (FMR) is a method to perform magnetic properties by detecting the motion of the magnetization in ferromagnetic sample [4]. The measurement signal is thermal magnetic noise which is related to the precession motion of magnetization in multiple magnetic thin films of read sensor. The tool for measurement is spectrum analyzer which displays in high range of frequency (GHz).

The previous study is reported that thermal magnetic noise is inversely proportional to the sensor volume [13] and [14]. As the size of magnetic read sensor keep shrinking, thermal magnetic noise becomes dominant and causes significant degradation of head signal-to-noise ratio (SNR). Because the signal voltage is a local correlation function of the magnetization in the free layer, reference layer, pinned layer, pinning layer and other magnetic layers. As a result, thermal magnetic noise can cause signal voltage fluctuation of magnetic read sensor. Thermal magnetic noise is performed the magnetization motion that can be theoretically studied by using the Landau-Lifshitz-Gilbert (LLG) equation as in [11], [15] and [16]. LLG equation is shown

in Equation 2.18, which describes the motion of a magnetization vector $\vec{M}$ in the presence of effective stiffness field $\vec{H}_{eff}$

$$\frac{d\vec{M}}{dt} = -\gamma\vec{M} \times \vec{H}_{eff} + \frac{\alpha}{M_s}\vec{M} \times \frac{d\vec{M}}{dt} \tag{2.18}$$

Here, $\vec{M}$ is the magnetization, M_s is saturation magnetization, γ is the gyromagnetic constant $\left(\gamma \approx 2.2 \times 10^5\, m/As\right)$, H_{eff} is effective stiffness field and α is the Gillbert damping constant. The damping parameter describes energy losses during precession (In term of mechanical analogy is closest to friction). Damping is determined by the material properties and defects. For example, if there is higher damping, it will result in larger resonance width that can indicates sensor defects. The Fig. 2.12 [8] shows the motion of the magnetization as it is described by the LLG equation. The first term of equation 2.18 represents the precession of magnetization around the effective stiffness field that provides the magnetic torque for the rotation of magnetization. The second term is the phenomenological damping that describes the energy dissipation as a function of the direction toward the effective field. After reaching the equilibrium state, the magnetization aligns itself along the direction of the effective stiffness field.

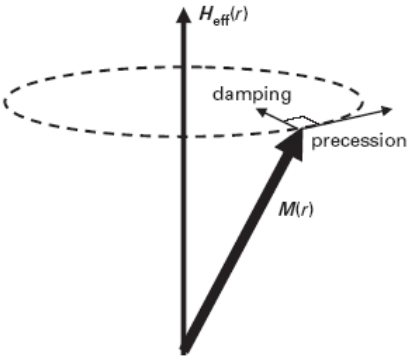

Fig. 2.12 The precession of the magnetization around the effective field according to the Landau-Lifshitz-Gilbert equation (LLG) [8]

The effective stiffness field is calculated by Equation 2.19 [11]

$$H_{eff,\phi} = H_{K,T}\cos 2\phi_0 + H_x \cos\phi_0 + H_y \sin\phi_0 \tag{2.19}$$

$H_{K,T}$ is the total anisotropy field resulted from crystalline and shape anisotropy terms by Equation 2.20 [11]. H_x is longitudinal field direction due to permanent

magnet. H_y is transverse field direction, which is perpendicular to free layer, due to external field. ϕ_0 is the angle between actual magnetization and ideal magnetization of free layer. When the magnetization of free layer is perpendicular to pinned/reference layer as ideal, ϕ_0 = 0,

$$H_{K,T} = \frac{2K_u}{\mu_0 M_s} + \left(N_y - N_x\right)M_s \tag{2.20}$$

K_u is crystalline anisotropy energy, μ_0 is permeability of free space, N_x and N_y are the effective demagnetization factors in the x (parallel track width) and y (stripe height) direction, respectively.

The magnetization fluctuation is measured by FMR spectrum analyzer that is displayed signal in range of frequency (GHz) as shown in Fig. 2.13 [17]. The key parameters are FMR frequency, FMR amplitude and FMR width at half maximum peak.

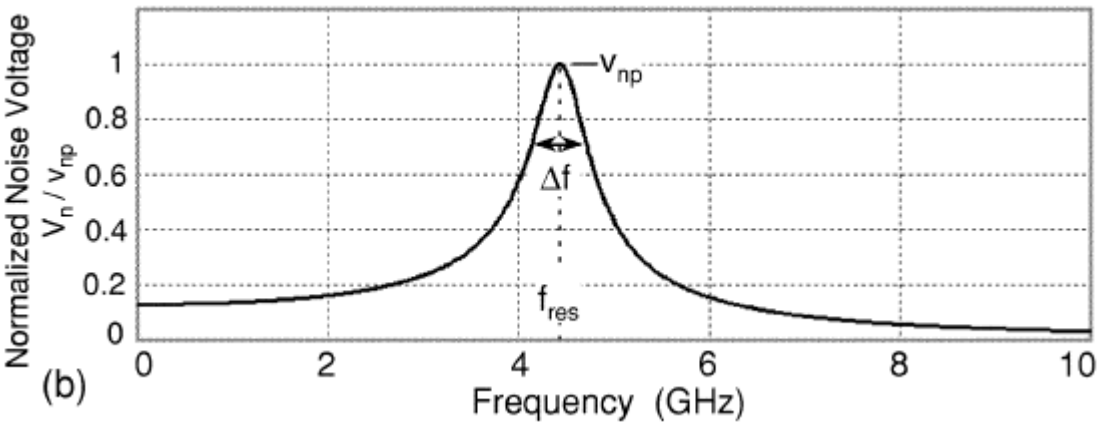

Fig. 2.13 Ferro magnetic resonance (FMR) spectrum [17]

The FMR frequency is determined by Equation 2.21 [17]

$$f_0 = \frac{\gamma}{2\pi}\sqrt{M_s H_{eff}} \tag{2.21}$$

FMR amplitude can be achieved from Equation 2.22 [17]

$$V_p = I\Delta R\cos\phi\sqrt{\frac{k_B T}{\alpha\mu_0\gamma M_s H_{eff} V\left(H_{eff} + M_s\right)}} \tag{2.22}$$

Where I is the measuring current, ΔR is the maximum resistance change, k_B is Boltzmann's constant ($k_B = 1.38 \times 10^{-23}$), T is absolute temperature, ϕ is the angle of magnetization between the free layer and the hard bias, V is the free layer volume.

Thermal electrical noise current that is associated with R is as Equation 2.23 [17]

$$i_n = \sqrt{\frac{4kT}{R}} = \sqrt{\frac{4kT\alpha\mu_0 M_s \Delta V}{\gamma}} \tag{2.23}$$

The FMR full width at half maximum of spectra peak (FMR width at 50% of the peak amplitude) is determined by the following equation [17]

$$\Delta f = \frac{\gamma}{2\pi}\alpha M_s \tag{2.24}$$

FMRA is a method to detect the magnetic property without destruction [4]. This tool is able to check the quality, sensitivity and instability of magnetic read sensor by layer-level state. Moreover, FMRA is used for analyze the effective stiffness field and damping which reflect the efficiency of magnetic read sensor. This useful information is not easy to study by the other methods. The FMR characteristic is related to magnetization fluctuation in different layer of magnetic read sensor. There are many reports [4], [14] and [18-22] that study on magnetic read sensor by using FMRA with varied reader design and varied condition composed of external magnetic field and bias voltage to check the magnetic property as following detail.

The work in [18] has been studied the thermal magnetic noise of Giant Magneto Resistive (GMR) head by varying aspect ratio (TW/SH) and strength of permanent magnet. The reduced track width by keeping the same aspect ratio and film thickness will not impact the FMR amplitude which results from accompanying increase of the demagnetization field within the sensing layer. While FMR frequency of narrower track width becomes significantly higher than the other one. However, the FMR spectrums show strongly functions to SH scale that are lower FMR amplitude and higher FMR frequency on shorter SH. In term of head stability, FMR characteristic is sensitive function of the permanent micro magnetic state at the abutted junction as in [18], [19] and [20]. The reference [20] shows FMR spectrum of TMR read sensor which has the correlation function of the magnetization motion in the free and reference layer. Both the magnetization motion of free and reference layers are greatly influenced by the strength of the bias field from the permanent magnets. In general, the magnetization motion of free layer is uncorrelated with

magnetization motion of reference layer. Therefore FMR spectrum is a superposition of the magnetization on free layer and reference layer. The paper [20] also present that there is stronger peak of FMR amplitude is attributed to a magnetization motion in the free layer. While a smaller feature at a slightly lower frequency is attribute from the magnetization motion in the pinned/reference layer.

There are the studied FMR behaviors that have changes with applied external magnetic field in transverse direction and current density as in [14], [21] and [22]. The references [14] and [21] suggest that in dynamic region of magnetic read sensor, the related FMR spectrum is determined by free layer magnetization fluctuation. While at high fields, magnetic read sensor is driven to have magnetization saturation and abnormal extremely is resonance with high amplitude than dynamic region. This condition is supposed that magnetization of free layer is nearly antiparallel to reference layer. The detailed analysis suggest that this resonance is due to the magnetization fluctuation in the reference/pinned layer.

In addition, FMR spectrum is able to detect the abnormal magnetic read sensor such as the potentially unstable sensor as in [4]. They present that FMR measurement allows to detect tilt of effective magnetization orientation of free layer. The result is shown the shift of FMR spectrum in two opposite directions of external field that is applied in transverse direction to permanent magnet. The source of free layer magnetization tilt may be the result of hard bias misalignment or domain structure, contribution of shape anisotropy and reference layer defects (or combination of these defects). The work in [14] shows multiple additional FMR peaks which are originated from polycrystalline nature of hard bias and cause inhomogeneity in the magnetization of free layer. The reference [7] shows abnormal increase in the FMR amplitude which performs before irreversible breakdown of magnetic read sensor. After the pinhole growth, the abnormal FMR amplitude is disappeared. The result is implying that related pinhole-free barrier. The result presents that spin transfer effect is not important for the presence of abnormal increased FMR amplitude via applying reversed current direction and vary measured current. It is very interesting to study the magnetic read sensor with various SH by using FMRA to more understand the magnetic property which is able to apply to extend the detection capabilities for magnetic recording industry.

Chapter 3
Methodology and Experiment

3.1 Introduction

This chapter presents a manufacturing process of magnetic head with sample specifications which are used to run the experiment. Next, FMRA and QST method are explained. Then the flow chart of the experiment is discussed; it is composed of detailed SH target, external magnetic field set up, volt bias set up and focused FMR and QST parameters. The experiment set up is explained in more details in the last section.

3.2 Manufacturing process of magnetic sensor

Figure 3.1 shows an outline of magnetic head production flow and process, composed of wafer process, bar process and slider process [3]. Wafer process is involved deposition, milling, cleaning and drying process which is completely defined read track width of read sensor. Next, wafer is sliced in bar level that results in bars with contained multiple sliders. Then, bar is lapped, which is referred to SH target. SH scale is significantly impact to read head sensitivity. It is very important to study the characteristic of magnetic read sensor in order to obtain optimized SH target for the yield of production with screening weak read ability.

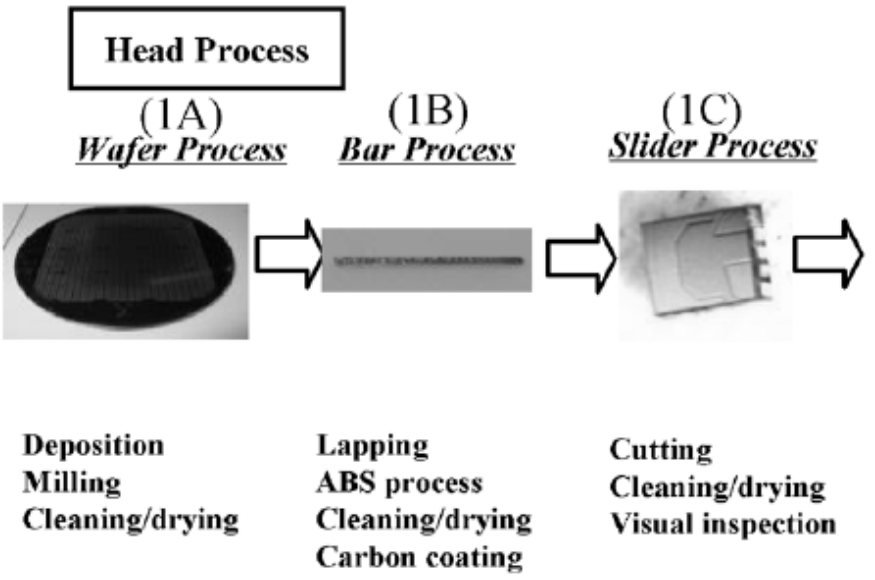

Fig. 3.1 Manufacturing process of magnetic head sensor [3]

After lapping process, bars are cleaning and drying then run diamond-like carbon (DLC) coating to prevent the corrosion. Next, bars are processed to make the air

bearing surface (ABS) by deposition, milling, cleaning and drying. After that, bars are run to QST to measure the electrical property. Finally, bars are machined for slider levels which are processed to cleaning and visual inspection. In this experiment, the samples are performed in bar level as FMR measurement is able to test on bar form. After lapping and DLC coating, bars were processed to test electrical property by using QST and magnetic property by using FMRA as shown in Fig. 3.2.

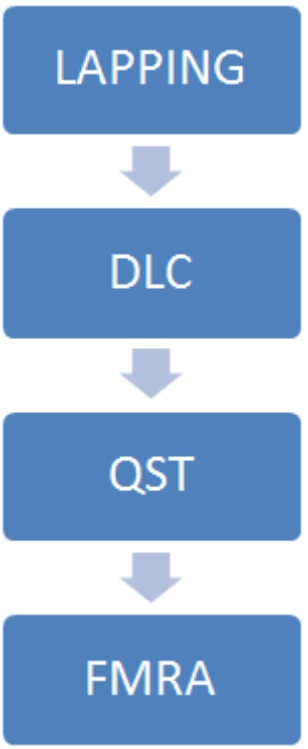

Fig. 3.2 Flow of experiment process

3.3 Sample specifications

The experiments were performed on TMR heads that were the same areal density and track width but different SH targets. This experiment had seven SH targets composed of shortest to longest SH as follows ; 20nm, -10nm, -5nm, nominal, +5nm, +10nm, +20nm. The SH scales were based on actual ranging work of TMR head in production.

3.4 Characterization Tools

The measurement was carried on bar level which FMRA and QST had test on the same sliders. FMR measurements were performed on bars equipped with high frequency probe. The system is provided thermal magnetic noise spectrum acquisition in the range of 0.3-10 GHz. The external magnetic field of arbitrary orientation which is transverse to cross-track is generated by quadrupole

electromagnet with up to 2500 Oe field magnitude. FMR spectra was captured for vary magnitude and angles of external field and spectra parameters were extracted by FMRA software. FMRA is a useful technique in the measurement of magnetic properties of ferromagnetic materials. This method measures magnetic property by detecting the motion of the magnetization in a ferromagnetic sample. As Fig. 3.3 [23], the applied static magnetic field H_0 that causes the total magnetic moment to precess around the direction of the local field H_{eff}, before relaxation processes damp this precession and the magnetization aligns with H_{eff}. If the sample is irradiated with a transverse RF field (microwaves of typically 1-35 GHz), and the RF frequency coincides with the precessional frequency, the resonance condition is fulfilled and the microwave power is absorbed by the sample. This precession occurs at the FMR frequency.

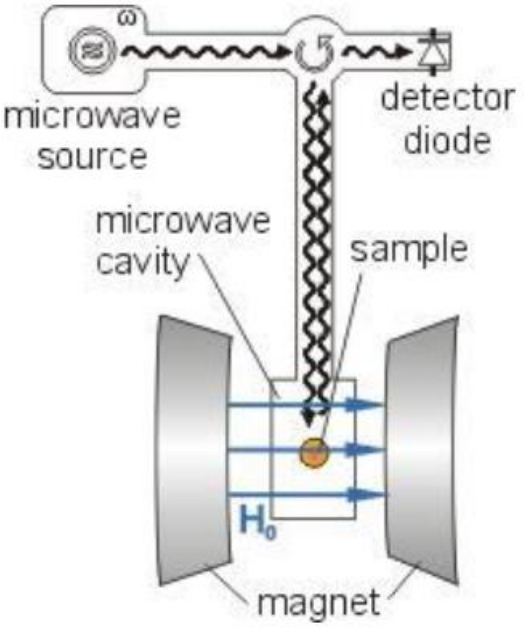

Fig. 3.3 Ferromagnetic resonance test [23]

The focused FMR parameters in this experiment were FMR frequency (f_0), FMR amplitude (V_p), FMR width (Δf) and secondary peaks. These parameters were referred the equation explained in chapter 2. FMRA is able to provide the explanation of magnetic properties of read sensor by layer-level state related to the efficiency of magnetic read head and not easy to find out with other method.

QST is a normal technique in the measurement of electrical properties that performs without flying head over a media to characterize whole performance of magnetic read sensor. This tool measures response of read sensor with applying external magnetic field in transverse direction by sweeping field from negative to

positive field. After that, transfer curve is gained which contains sensitivity and instability information. The focused QST parameters in this experiment were amplitude, asymmetry, SNR, MRR, Bark jump and hysteresis.

3.5 Flow chart of the experiment

The flow chart of the experiment shows in Fig. 3.4. The measurements were performed on TMR heads with the same track width but different SH targets in bar level. Total sample was 14 bars contained 50 sliders per bar. There were divided 2 bars per SH target. Total sliders per SH target were 100 sliders. The experiments were applied with external magnetic field both longitudinal and transverse direction with varying set up of volt biases as shown in Table 3.1. The detailed conditions of experiment were explained as follows:

3.4.1 The experiment was performed on FMRA without applying external magnetic field to examine behavior of free layer with various SH scales.

3.4.2 The external magnetic field was applied in longitudinal direction which was parallel to permanent magnet direction. The longitudinal fields were applied with forward and reverse directions composed of +1.2 kOe and -1.2 kOe. The external magnetic field in longitudinal direction was to characterize the behavior of free layer and permanent magnet with various SH scales.

3.4.3 The external magnetic field was applied in transverse direction which was perpendicular to permanent magnet direction. The transverse fields were applied with same magnitude with opposite polarities composed of +520 Oe and -520 Oe. This was to research the symmetry of magnetic read sensor with various SH scales.

3.4.4 QST was applied with external magnetic field in transverse direction. The transverse fields were applied with same magnitude with opposite polarities composed of +520 Oe and -520 Oe. Then transfer curve was gained with sensitivity and instability parameters which were looked into electrical properties.

All the experiments were conducted with two levels of volt biases composed of 140mV and 160mV in forward and reverse directions in order to investigate the effect of heat and also the switching time of the magnetic read sensor in both directions. The FMRA was used to characterize the magnetic properties of read sensor by layer-level state with varied SH targets that were under condition of varied external magnetic fields and volt biases. The behavior of FMR spectrum corresponds to magnetization of free layer, pinned layer and permanent magnet which are related to the read ability of magnetic read sensor. In term of QST, it was used to analyze of electrical properties of magnetic read sensor.

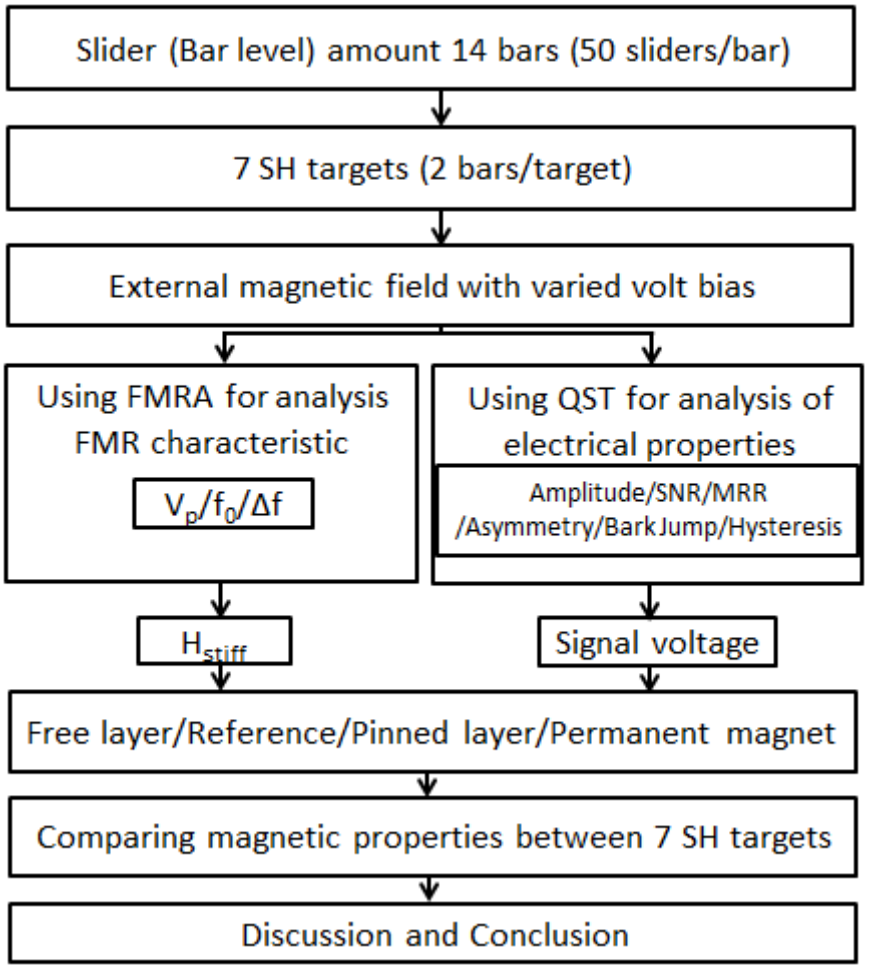

Fig. 3.4 Flow chart of the experiment

Table 3.1 The experimental set up

Tool	External magneitc field	Direction of external magnetic	Bias Voltage			
FMRA	No external field	-	140mV	-140mV	160mV	-160mV
	+/-1200 Oe	Longitudinal				
	+/-520 Oe	Transverse				
QST	+/-520 Oe	Transverse				

Chapter 4
Experimental Results

4.1 Introduction

The evaluation was focused on TMR read sensor behavior with the same track width but different SH targets (-20nm, -10nm, -5nm, nominal, +5nm, +10nm, +20nm) by using ferromagnetic resonance analyzer (FMRA) and quasi-static test (QST). The FMRA was applied external magnetic field on both longitudinal and transverse directions to permanent magnet with varied set up of volt biases in order to study the magnetic properties of read sensor with multiple SH by layer-level state. The QST was applied external magnetic field in transverse direction to permanent magnet used to explain the electrical properties of magnetic read sensor.

This chapter presents the result of TMR read sensor characterization with various SH scales that are composed of three sections. First section is explained about FMR spectrum without applying external magnetic field. Next section is illustrated about the result of FMR spectrum with applying external magnetic field in longitudinal to permanent magnet direction. Last section presents the FMR spectrum with applying external magnetic field in transverse direction.

4.2 FMR spectrum as a function of no external magnetic field

Magnetic read sensors with multi-stripe height were performed on FMR measurement without applying external magnetic. The SH scales were composed of -20nm, -10nm, -5nm, nominal, +5nm, +10nm, +20nm SH targets. The volt bias were applied with two levels in forward and reverse directions composed of +140mV, -140mV, +160mV and -160mV. This experiment was studied on FMR spectrum of TMR read head with varying SH scales in the GHz range. Y-axis is the FMR amplitude (nV) and X-axis is the FMR frequency (GHz).

Figure 4.1 shows a FMR spectrum on magnetic read sensor with the shortest SH target and longest SH target without applying external magnetic field and bias with +140 mV voltage. The shortest SH target was -20nm SH from nominal as illustrated in Fig. 4.1 (a). The longest SH target was +20nm SH from nominal as shown in Fig. 4.1 (b). For the shortest SH, FMR amplitude was 1.11 nV and FMR frequency was 8.09 GHz. While the longest SH, FMR amplitude was increased to 8.29 nV and FMR frequency was shifted down to 4.82 GHz. The shorter SH of magnetic read sensor exhibited lower FMR amplitude with higher FMR frequency than the longer one.

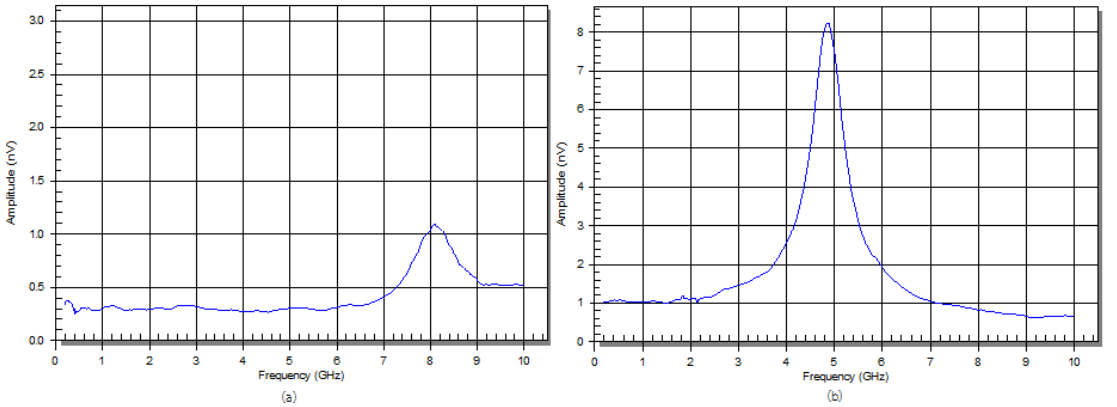

Fig. 4.1 FMR spectrum without applying external magnetic field with +140 mV volt bias for two different SH targets of TMR sensor (a) shortest SH target is -20nm SH from nominal (b) longest SH target is +20nm SH from nominal

Table 4.1 shows the summary of FMR result for magnetic read sensor between all seven SH targets without applying external magnetic field and varied set up of volt biases. The results showed decreasing in FMR amplitude with increasing in FMR frequency and FMR resonance width as the SH was shorter. These results were plotted as shown in Fig. 4.2 referred to Table 4.1 that was FMR data summary of magnetic read sensor with various SH scales and applying no external magnetic field.

Table 4.1 Summary of the FMR result for magnetic read sensor with seven SH targets from -20nm SH to +20nm SH target without applying external magnetic field

Parameter	Volt Bias	SH TGT						
		-20nm	-10nm	-5nm	Nominal	+5nm	+10nm	+20nm
FMR Amplitude (nV)	140mV	1.11	2.16	3.14	3.98	4.74	6.35	8.29
	-140mV	1.20	2.46	3.34	4.33	5.13	6.82	8.31
	160mV	1.23	2.51	3.50	4.52	5.42	7.23	9.71
	-160mV	1.36	2.91	3.88	5.02	5.91	8.02	8.84
FMR Frequency (GHz)	140mV	8.09	6.85	6.37	6.04	5.64	5.16	4.82
	-140mV	8.01	6.80	6.35	5.99	5.60	5.23	4.72
	160mV	8.08	6.82	6.37	6.00	5.59	5.19	4.81
	-160mV	7.99	6.85	6.36	6.00	5.59	5.17	4.65
FMR Resonance Width (GHz)	140mV	0.91	0.74	0.68	0.65	0.63	0.58	0.56
	-140mV	0.85	0.65	0.62	0.59	0.60	0.56	0.55
	160mV	0.89	0.76	0.68	0.67	0.64	0.59	0.55
	-160mV	0.84	0.66	0.61	0.60	0.58	0.56	0.53

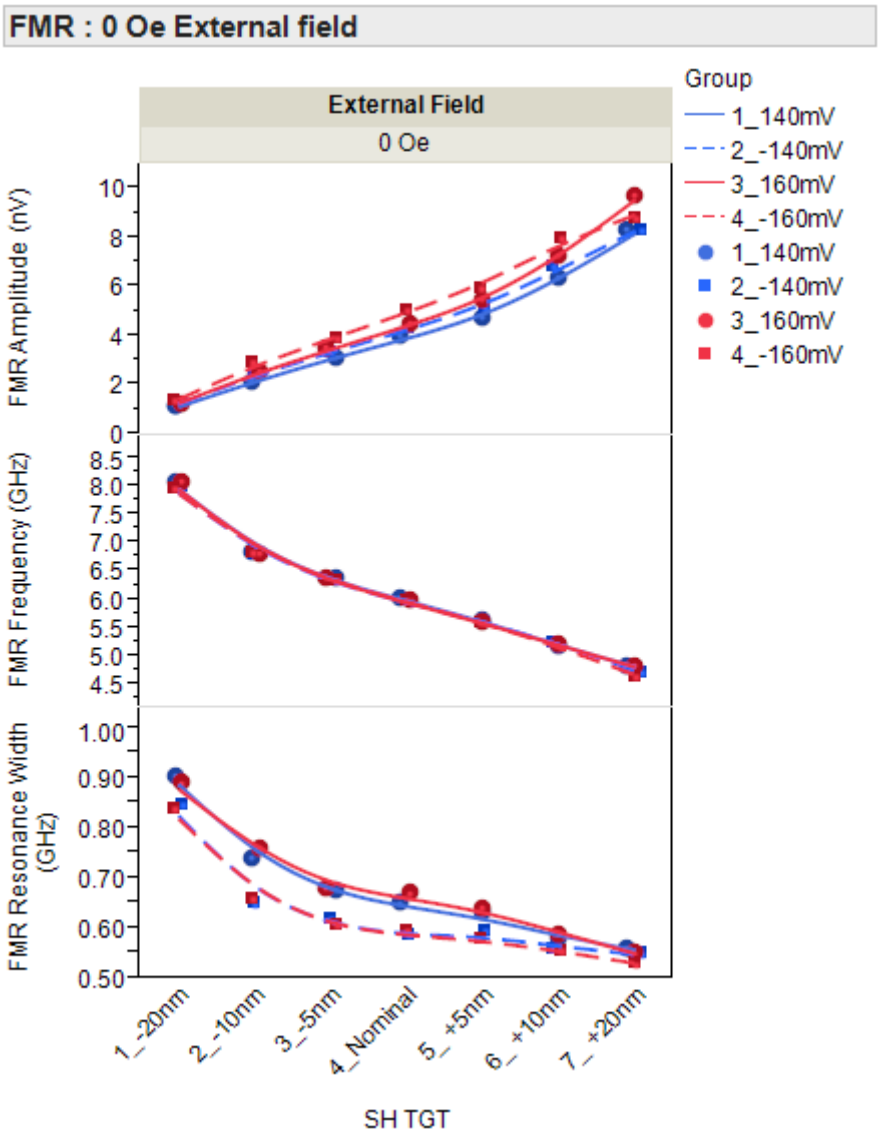

Fig. 4.2 FMR spectrum trend of magnetic read sensor with various SH targets without applying external magnetic field and varied set up of volt biases

Under no external magnetic field condition, it appears that the behavior of FMR spectrum has depended on SH scale. FMR spectrum of each SH scale can be well attributed to the magnetization fluctuation of the free layer which is referred from [4], [20] and [21]. As the effective stiffness field is proportional related to FMR frequency as shown in Equation 2.21 and is inversely associated with FMR amplitude as shown in Equation 2.22. It suggests that at the shorter SH the effective stiffness field of free layer has increased according to the result of increasing FMR frequency and decreasing FMR amplitude trend as illustrated in Fig. 4.2. The experiments show that the fluctuation of stiffness field in free layer with various SH scales has resulted from changed shape anisotropy as explained in Equation 2.19 and Equation 2.20.

These finding imply that SH scale plays some roles on the effective stiffness field of free layer which has an effect on read ability of magnetic read sensor.

All set up of volt biases composed of +140mV, -140mV, +160mV and -160mV showed the same trend of FMR spectrum in varying SH scales that were decreasing in FMR amplitude, increasing in FMR frequency and FMR resonance width as the SH was shorter. The forward volt bias, FMR spectrum with +160mV volt bias on the shortest and longest SH targets are shown in Fig. 4.3. This volt bias displayed higher FMR amplitude but comparable FMR frequency and FMR resonance width compared to +140mV volt bias as illustrated in Fig. 4.2. These results showed the same trend for all SH scales.

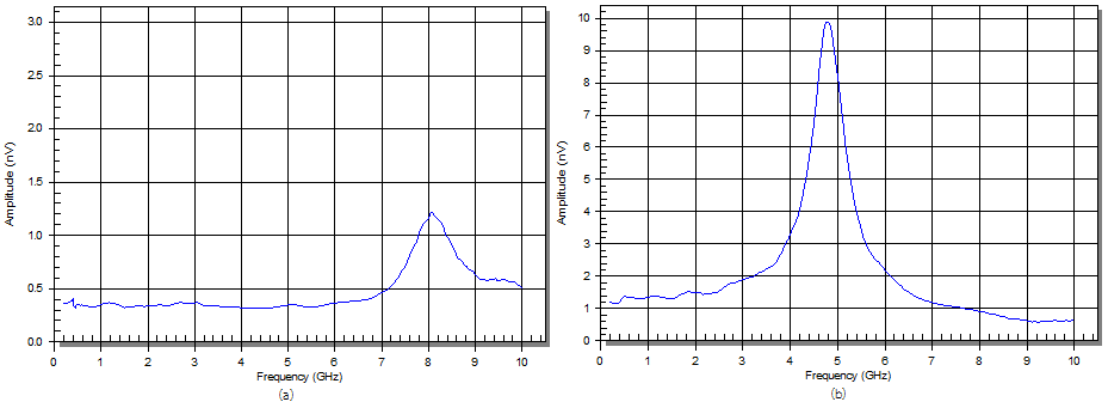

Fig. 4.3 FMR spectrum without applying external magnetic field with +160 mV volt bias for two different SH targets of TMR sensor (a) shortest SH target is -20nm SH from nominal (b) longest SH target is +20nm SH from nominal

In term of reverse volt bias, The FMR spectrum with -140mV and -160mV volt bias on the shortest and longest SH targets are shown in Fig. 4.4 and Fig. 4.5. The comparison between these two levels of reverse volt bias was the same trend as forward volt bias. The -160mV volt bias showed higher FMR amplitude but comparable FMR frequency and FMR resonance width compared to -140mV volt bias. The higher level of volt bias in forward and reverse direction has associated with increased FMR amplitude as explained by Equation 2.22. This study demonstrates that the level of volt bias has had an effect on FMR spectrum detected by parameter of FMR amplitude.

At same level of volt bias, +140mV volt bias showed slightly lower FMR amplitude with comparable FMR frequency compared to -140mV volt bias. While FMR resonance width significantly displayed higher on +140mV forward volt bias as shown in Fig. 4.2. The comparison between +160mV and -160mV volt bias was the same trend as the comparison between +140mV and -140mV volt bias which showed slightly lower FMR amplitude and comparable FMR frequency but higher

FMR resonance width on forward volt bias. It seems that forward volt bias has presented higher damping than reverse volt bias due to higher FMR resonance width. These results can be explained by Equation 2.24 which its damping is closely related to FMR resonance width. The study suggests that direction of volt bias has an effect on damped oscillations of magnetic material as demonstrated in [24]. It has been established that spin-transfer torque in TMR head induces magnetization switching from parallel to antiparallel and antiparallel to parallel also depended on the direction of volt bias [25]. Hence, these experiments demonstrate that forward volt bias has performed better switching time of magnetization than reverse volt bias which is detected by higher damping from parameter of FMR resonance width.

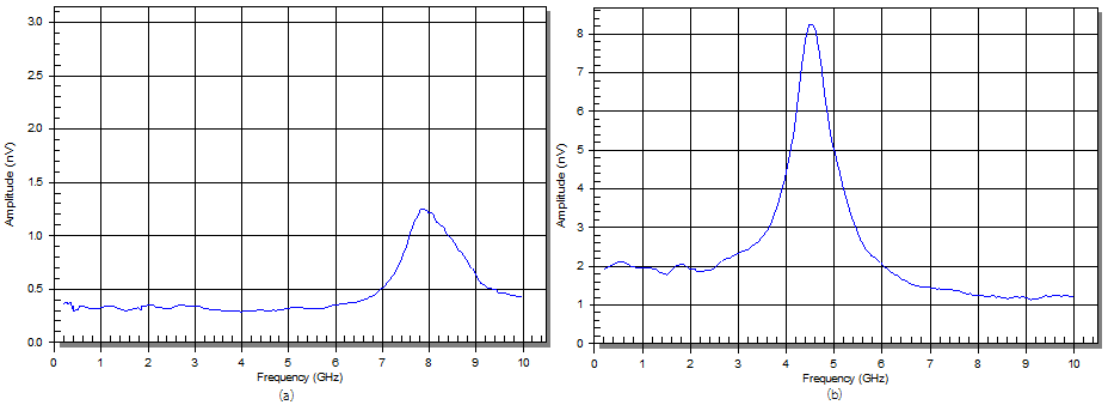

Fig. 4.4 FMR spectrum without applying external magnetic field with -140 mV volt bias for two different SH targets of TMR sensor (a) shortest SH target is -20nm SH from nominal (b) longest SH target is +20nm SH from nominal

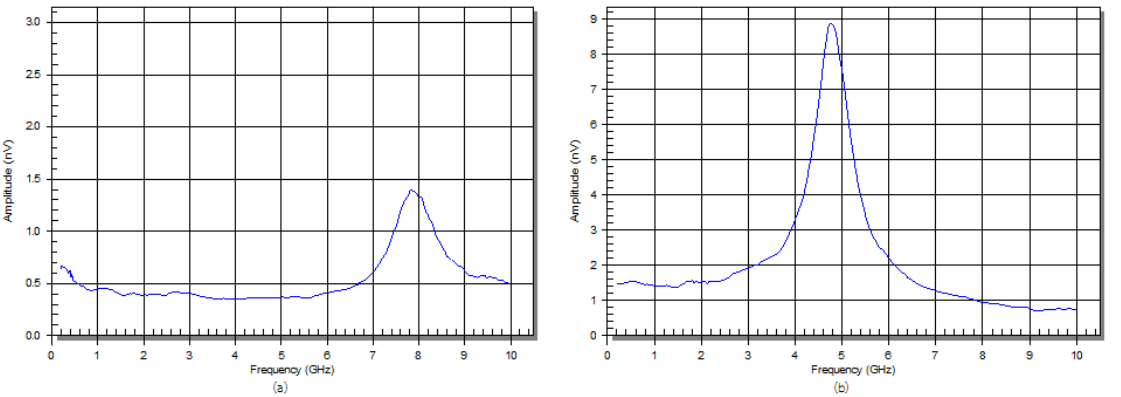

Fig. 4.5 FMR spectrum without applying external magnetic field with -160 mV volt bias for two different SH targets of TMR sensor (a) shortest SH target is -20nm SH from nominal (b) longest SH target is +20nm SH from nominal

Under applying no external magnetic field, the behavior of FMR spectrum has depended on SH scale and the effect of heat has been indicated by FMR amplitude

while direction of volt bias has been detected by FMR resonance width. These results have been based on FMR measurement which has required to analysis together with QST results as follows.

Magnetic read sensors with multi-stripe height performed on QST with applying external magnetic field in transverse direction to permanent magnet and varied set up of volt biases as conducted by FMR measurement. Table 4.2 shows QST results for all seven SH targets with varied set up of volt biases. For the shortest SH target that was -20nm SH from nominal with +140mV volt bias, amplitude was around 8 mV, asymmetry sigma was 8.8% and SNR was 16.8% as indicated in Table 4.2. The transfer curve with +140mV volt bias of the shortest SH shows in Fig. 4.6 (a). The Y-axis of transfer curve is amplitude (μV) and X-axis is the transverse magnetic field (Oe). Transfer curve is resulted from the transverse field applying with same magnitude but opposite polarities composed of +520 Oe and -520 Oe.

Table 4.2 Summary of the QST result between -20nm SH to +20nm SH targets

BQST	Volt Bias	SH TGT						
		-20nm	-10nm	-5nm	Nominal	+5nm	+10nm	+20nm
Amplitude (uV)	140mV	8036.6	9775.0	10523.0	11367.5	12060.0	12596.4	13118.3
	-140mV	7954.4	9787.3	10592.9	11084.0	11632.6	12695.0	12943.6
	160mV	8907.9	10658.6	11649.1	12695.0	13173.8	14040.9	14562.9
	-160mV	8961.3	10597.0	11671.7	12612.8	13151.2	14008.0	14279.3
MRR (ohm)	140mV	763.2	603.9	543.7	496.8	464.3	412.7	363.0
	-140mV	734.5	590.5	531.8	487.5	452.2	406.7	359.9
	160mV	752.9	598.9	537.9	493.2	459.8	410.0	361.6
	-160mV	730.1	585.7	528.9	486.9	449.8	404.4	358.5
SNR (dB)	140mV	16.84	20.46	22.16	23.36	24.27	25.62	26.69
	-140mV	16.90	20.63	22.51	23.42	24.49	25.72	26.88
	160mV	17.76	21.28	23.10	24.34	25.09	26.35	27.38
	-160mV	18.02	21.43	23.28	24.44	25.11	26.38	27.35
Asymmetry-sigma (%)	140mV	8.82	5.92	10.37	12.33	10.89	10.90	20.48
	-140mV	11.10	10.17	10.35	11.71	9.48	14.53	16.05
	160mV	10.09	7.91	13.06	13.50	11.75	12.08	18.50
	-160mV	9.66	8.58	8.83	9.73	9.55	12.54	13.46
Bark Jump (%)	140mV	4.03	3.31	2.98	2.90	3.15	2.77	2.69
	-140mV	4.11	3.21	3.15	2.82	3.18	2.61	2.59
	160mV	4.10	3.67	3.36	3.02	3.26	2.81	2.86
	-160mV	4.05	3.62	3.28	3.04	3.34	2.72	2.82
Hysteresis (%)	140mV	3.78	2.96	3.33	2.81	2.85	2.88	2.59
	-140mV	3.78	3.10	2.92	2.58	2.95	2.34	2.33
	160mV	4.08	3.59	3.19	2.80	2.79	2.89	2.74
	-160mV	3.86	3.09	3.06	2.72	2.93	2.59	2.62

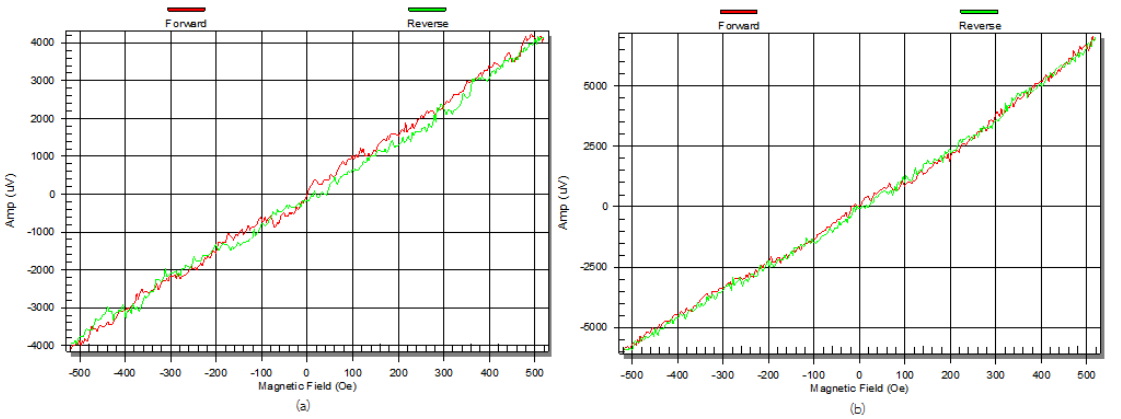

Fig. 4.6 Transfer curve of magnetic read sensor with +140 mV volt bias for two different SH targets of TMR sensor (a) shortest SH target is -20nm SH from nominal (b) longest SH target is +20nm SH from nominal

For the longest SH target (+20nm SH from nominal), amplitude was increased to 13.1 mV, asymmetry sigma was wider to 20.5% and SNR was increased to 26.7 dB as indicated in Table 4.2. Figure 4.6 (b) is the transfer curve of the longest SH target. The shorter SH exhibited lower amplitude and SNR but better asymmetry than the longer one as shown in Fig. 4.6 (a) and Fig. 4.6 (b). The instability parameters composed of Barkhausen Jump and hysteresis were worse at the shortest SH as illustrated in Fig. 4.6 (a).

Figure 4.7 shows QST trend of magnetic read sensor of all seven SH targets from -20nm SH target to +20nm SH target that is referred to Table 4.2. All set up of volt biases had the same QST trend that showed decreasing amplitude and SNR trend as the SH was shorter. While MRR was increasing trend due to reduced resistance area as shrinking SH scale. In term of the symmetry performance was better as the SH was shorter. While instability parameters composed of Barkhausen Jump and hysteresis showed negative result at the shorter SH. These QST results demonstrated less sensitivity, better symmetry and worse instability parameters at the shorter SH which had an effect on read ability of magnetic read sensor. The study suggests that overlapping has been better than underlapping because it is more symmetry at the shorter SH. The SH limit by QST show that it should not be over +20nm from nominal as indicated in Fig. 4.7. Lapping process can use this SH limit to screening bad material which is worse electrical properties from production.

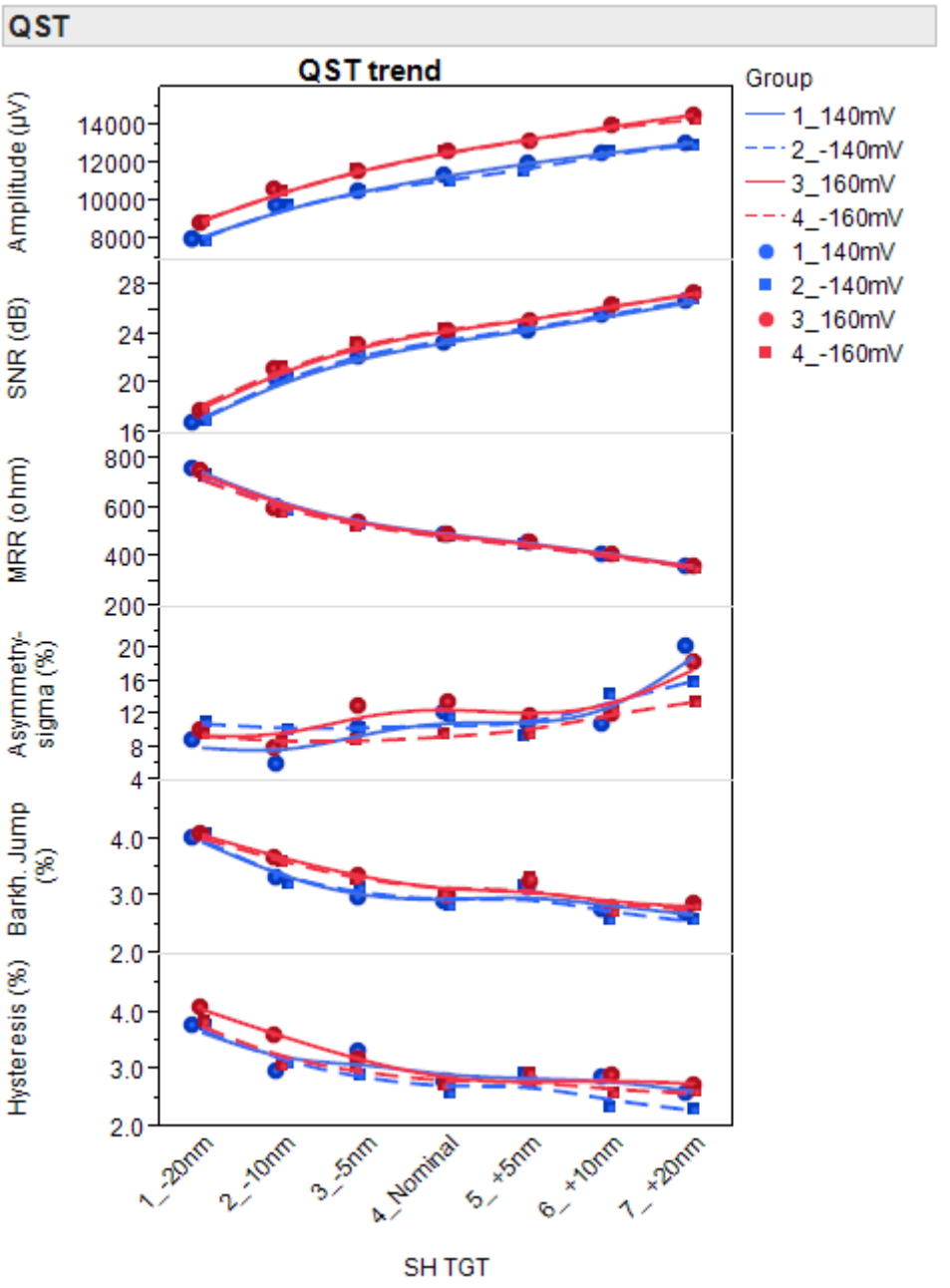

Fig. 4.7 QST trend of magnetic read sensor with various SH scales from -20nm SH target to +20nm SH target

The forward volt bias, +160mV volt bias showed higher amplitude and SNR with worse asymmetry and instability parameters compared to +140mV volt bias as demonstrated in Fig. 4.7. These results showed the same trend for all SH scales. The transfer curve of the shortest and longest SH targets with +160mV volt biases are shown in Fig. 4.8. In term of reverse volt bias, the transfer curve of the shortest and longest SH with -140mV and -160mV volt biases are shown in Fig. 4.9 and Fig. 4.10, respectively. The comparison between these two levels of reverse volt bias was the

same trend as forward volt bias. The -160 mV volt bias showed higher amplitude and SNR with worse asymmetry and instability parameters compared to -140mV volt bias.

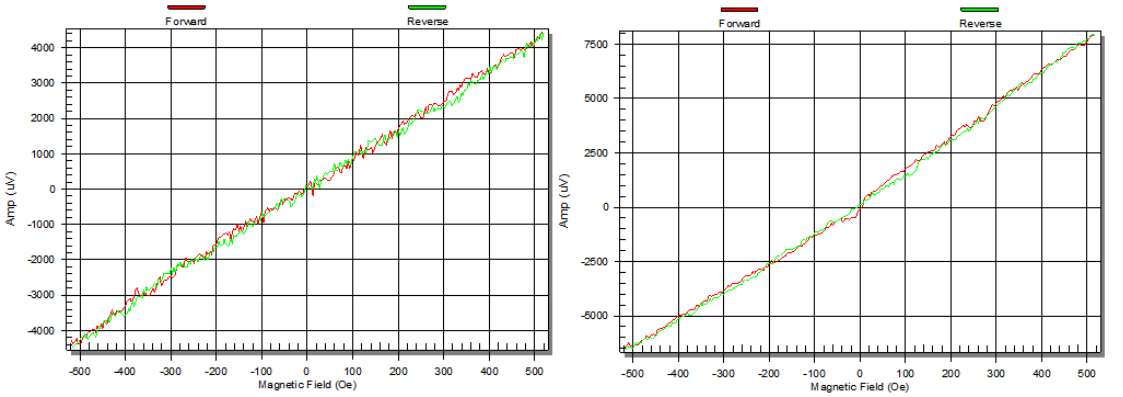

Fig. 4.8 Transfer curve of magnetic read sensor with +160 mV volt bias for two different SH targets of TMR sensor (a) shortest SH target is -20nm SH from nominal (b) longest SH target is +20nm SH from nominal

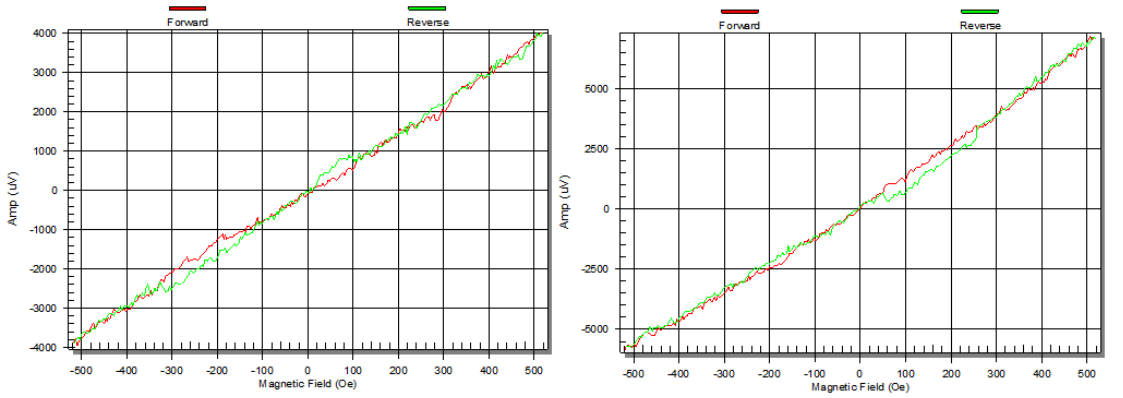

Fig. 4.9 Transfer curve of magnetic read sensor with -140 mV volt bias for two different SH targets of TMR sensor (a) shortest SH target is -20nm SH from nominal (b) longest SH target is +20nm SH from nominal

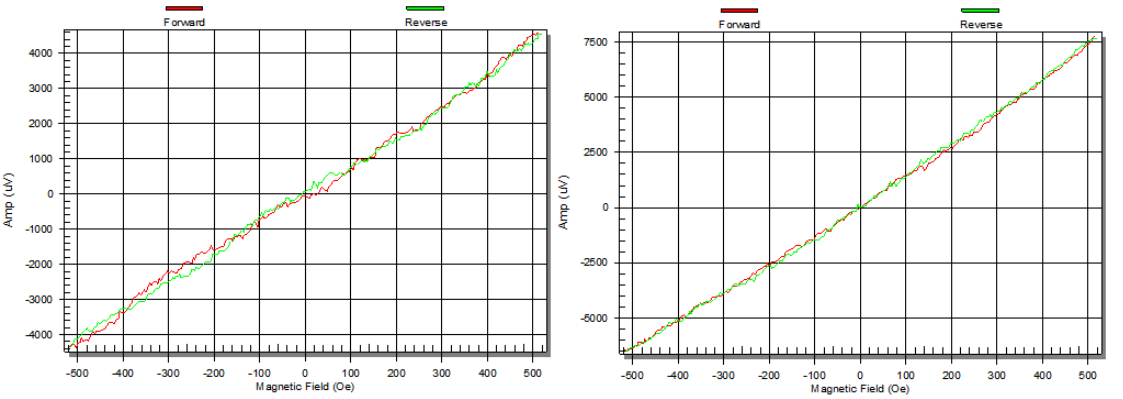

Fig. 4.10 Transfer curve of magnetic read sensor with -160 mV volt bias for two different SH targets of TMR sensor (a) shortest SH target is -20nm SH from nominal (b) longest SH target is +20nm SH from nominal

Higher level of volt bias in forward and reverse directions has correlated with increased amplitude and SNR with worse instability as shown in Fig. 4.7. This study demonstrates that the level of volt bias can be detected by QST result. At same magnitude of volt bias, +140mV volt bias showed comparable QST results compared to -140mV volt bias. The comparison between +160mV and -160mV volt bias was the same trend as the comparison between +140mV and -140mV volt bias presented comparable QST performance between forward and reverse directions as shown in Fig. 4.7. The effect of heat has resulted to higher sensitivity and worse instability while direction of volt bias has no impact on QST performance. As combination FMR and QST result, it is found that at the shorter SH the effective stiffness field of free layer has increased trend. This can be observed through the trend of increasing in FMR frequency and decreasing in FMR amplitude. QST result has corresponded to the stiffness field trend that shows less sensitivity and SNR as the SH is shorter.

According to correlated function between SH and effective stiffness field, FMR frequency related to stiffness field has shown good correlation to MRR as illustrated in Fig. 4.11. This MRR is closely related to SH scale varied for study the FMR behavior. The higher FMR frequency has been found as MRR is higher or SH scale is shorter. It appears that amplitude and SNR have been inversely related to FMR frequency as shown in Fig. 4.12 and Fig. 4.13. The lower amplitude and SNR trend have been found as FMR frequency is higher. It would be interesting to estimate spec some important QST parameters of magnetic read sensor by using the FMR parameters that is able to enhance its detection capabilities for magnetic recording industry.

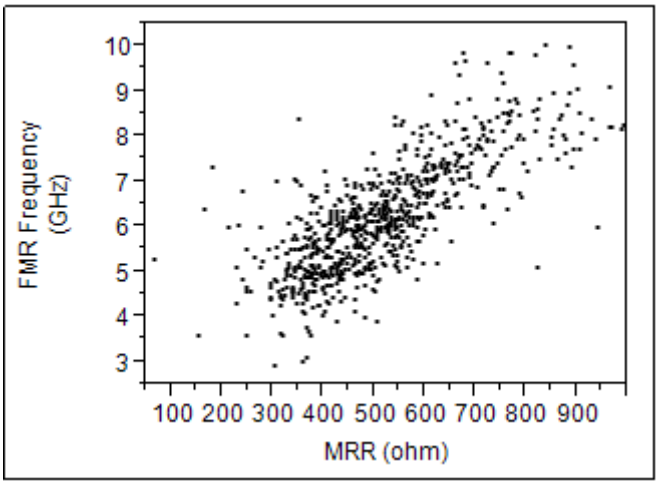

Fig. 4.11 Correlation between FMR frequency and MRR at QST

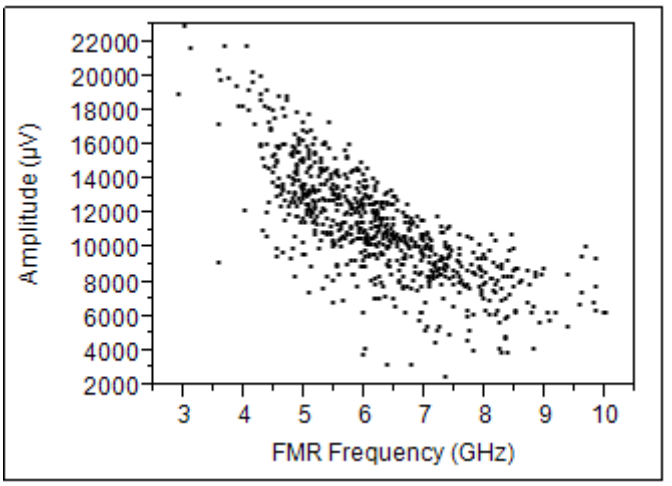

Fig. 4.12 Correlation between FMR frequency and amplitude at QST

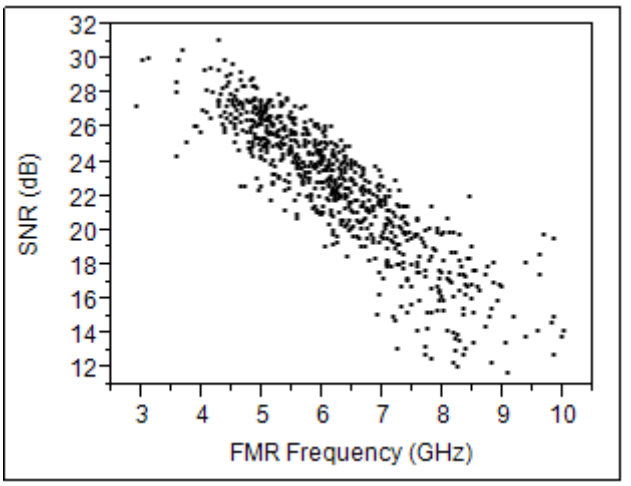

Fig. 4.13 Correlation between FMR frequency and SNR at QST

4.3 Longitudinal field dependence of the FMR spectrum

The longitudinal external magnetic field was applied along the magnetic read sensor width that was parallel to the permanent magnet direction. The longitudinal field was applied both forward and reverse direction composed of +1.2 kOe and -1.2 kOe. The experiments were conducted with two levels of volt biases in forward and reverse directions which were the same set up as first condition with applying no external magnetic field. The volt biases were composed of 140mV and 160mV volt bias.

Figure 4.14 shows a FMR spectrum on magnetic read sensor of two different SH targets with applying +1.2 kOe external magnetic field and +140 mV volt bias. The FMR spectrum of the shortest SH target (-20nm SH from nominal) is illustrated in Fig. 4.14 (a). The FMR spectrum of the longest SH target (+20nm SH from nominal) is shown in Fig. 4.14 (b). For the shortest SH, FMR amplitude was 1.02 nV, FMR frequency was 7.02 GHz and FMR resonance width was 0.85 GHz. For the longest SH, FMR amplitude slightly increased to 2.36 nV, FMR frequency slightly shifted down to 6.34 GHz and FMR resonance width was slightly wider to 0.97 GHz**.** The FMR amplitude, frequency and resonance width showed slightly difference between the shortest and longest SH. However, for the longest SH a secondary FMR peak in high frequency was found as shown in Fig. 4.14 (b). This additional FMR peak did not appear in the shortest SH as shown in Fig. 4.14 (a). The other set up of volt biases composed of -140mV, +160mV and -160mV also found the secondary FMR peak in high frequency at the longest SH as illustrated in Fig. 4.15 (b), Fig. 4.16 (b) and Fig. 4.17 (b).

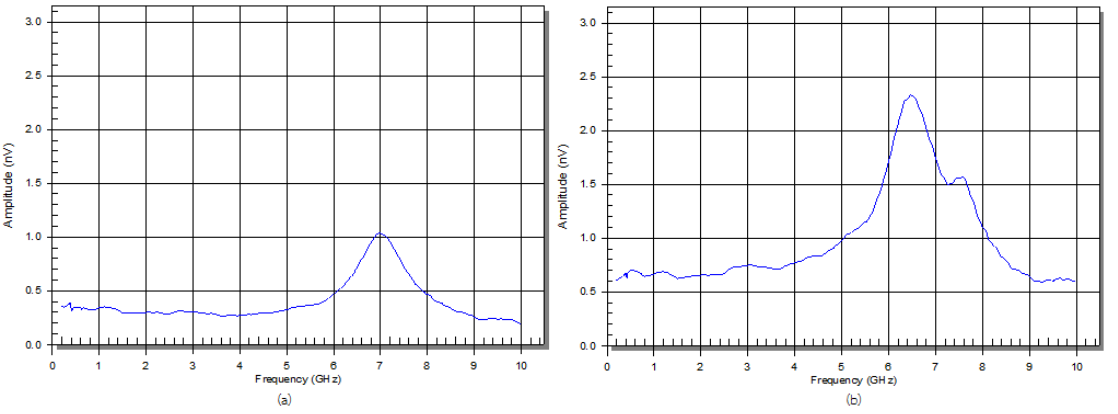

Fig. 4.14 FMR spectrum with applying +1.2 kOe external magnetic field with +140 mV volt bias for two different SH targets of TMR sensor (a) shortest SH is -20nm SH from nominal (b) longest SH is +20nm SH from nominal

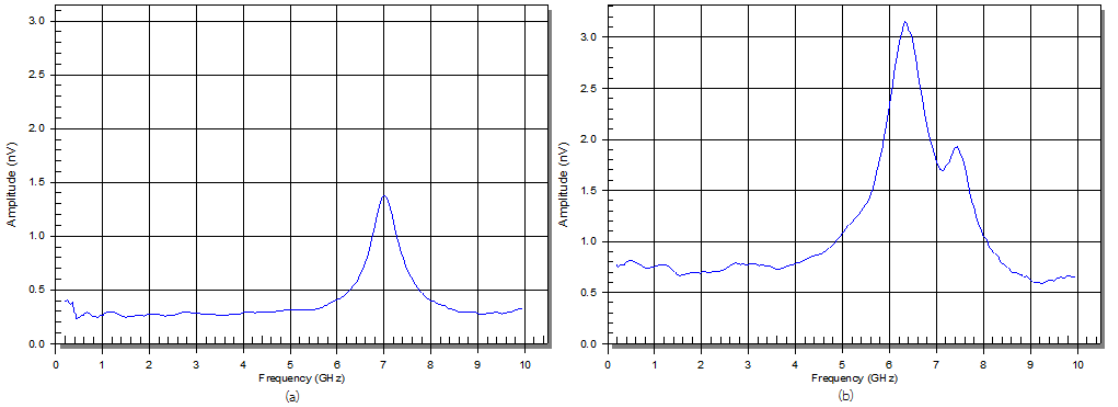

Fig. 4.15 FMR spectrum with applying +1.2 kOe external magnetic field with -140 mV volt bias for two different SH targets of TMR sensor (a) shortest SH target is -20nm SH from nominal (b) longest SH is +20nm SH from nominal

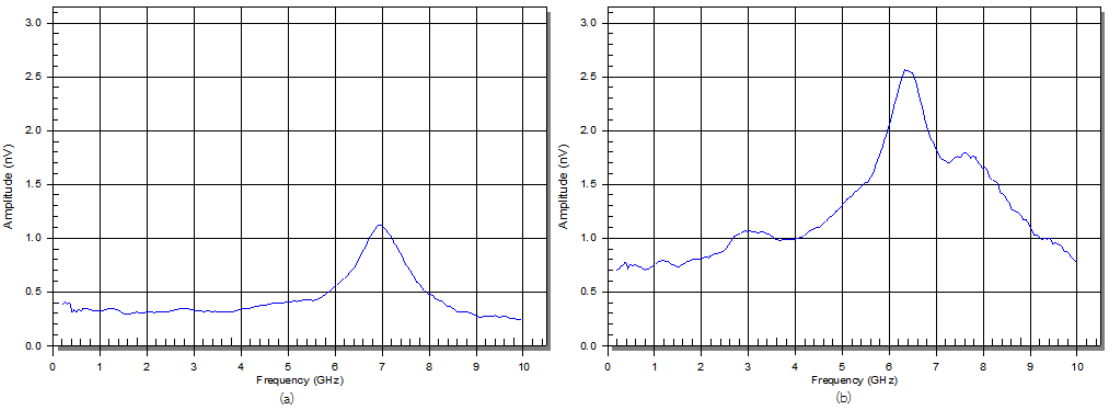

Fig. 4.16 FMR spectrum with applying +1.2 kOe external magnetic field with +160 mV volt bias for two different SH targets of TMR sensor (a) shortest SH target is -20nm SH from nominal (b) longest SH target is +20nm SH from nominal

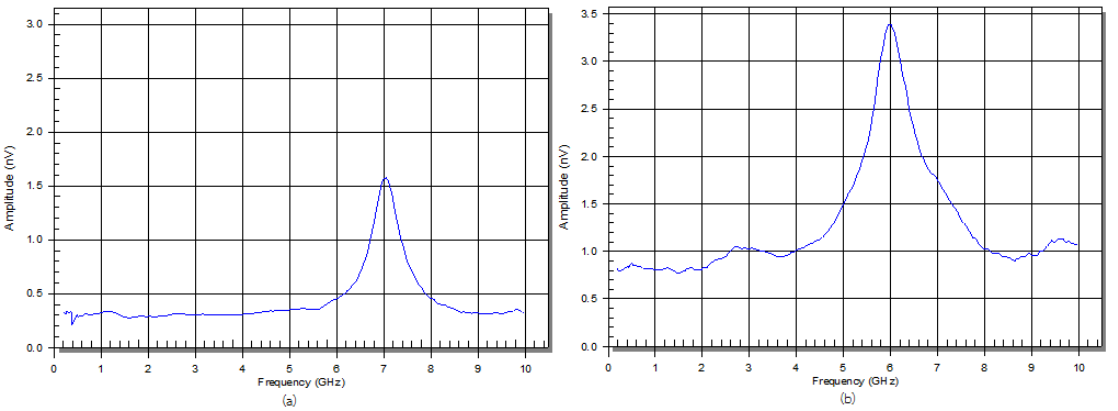

Fig. 4.17 FMR spectrum with applying +1.2 kOe external magnetic field with -160 mV volt bias for two different SH targets of TMR sensor (a) shortest SH target is -20nm SH from nominal (b) longest SH target is +20nm SH from nominal

Table 4.3 shows the summary of FMR result for magnetic read sensor between all seven SH targets (-20nm, -10nm, -5nm, nominal, +5nm, +10nm, +20nm) with varied set up of volt biases and applying with +1.2 kOe applying external magnetic field. The FMR results showed slightly decreased FMR amplitude and FMR resonance width with slightly increased FMR frequency as the SH was shorter. These finding were plotted in Fig. 4.18 referred from Table 4.3 that showed the trend of FMR spectrum of magnetic read sensor with various SH scales with applying +1.2 kOe external magnetic fields. There were a slightly changing of FMR spectrum in various SH scales. It seems that the behavior of FMR spectrum did not depend on SH scale as previous condition that applying no external magnetic field.

Table 4.3 Summary of the FMR result for magnetic read sensor with seven SH targets from -20nm SH to +20nm SH target with +1.2 kOe applying external magnetic field

External field	+1.2 kOe							
Parameter		SH TGT						
	Volt Bias	-20nm	-10nm	-5nm	Nominal	+5nm	+10nm	+20nm
FMR Amplitude (nV)	140mV	1.02	1.25	1.43	1.64	1.75	1.84	2.36
	-140mV	1.39	1.74	1.87	2.24	2.41	2.62	3.30
	160mV	1.07	1.40	1.55	1.80	1.92	2.02	2.60
	-160mV	1.59	2.07	2.14	2.70	2.80	3.08	3.43
FMR Frequency (GHz)	140mV	7.02	6.98	6.87	6.79	6.76	6.48	6.34
	-140mV	7.05	6.97	6.83	6.76	6.74	6.45	6.25
	160mV	6.98	6.98	6.79	6.77	6.77	6.50	6.34
	-160mV	7.09	6.98	6.79	6.73	6.72	6.45	6.07
FMR Resonance Width (GHz)	140mV	0.85	0.98	1.01	1.06	1.04	1.05	0.97
	-140mV	0.67	0.79	0.79	0.79	0.82	0.78	0.78
	160mV	0.88	1.01	1.03	1.08	1.06	1.06	1.02
	-160mV	0.66	0.72	0.76	0.76	0.80	0.77	0.73

All set up of volt biases composed of +140mV, -140mV, +160mV and -160mV demonstrated the same trend of FMR spectrum in various SH scales. The results showed slightly changing of FMR amplitude, FMR frequency and FMR resonance width as the SH was shorter. These results indicate that the high external magnetic field has driven the free layer to the magnetization saturation as studied in [14] and [21].

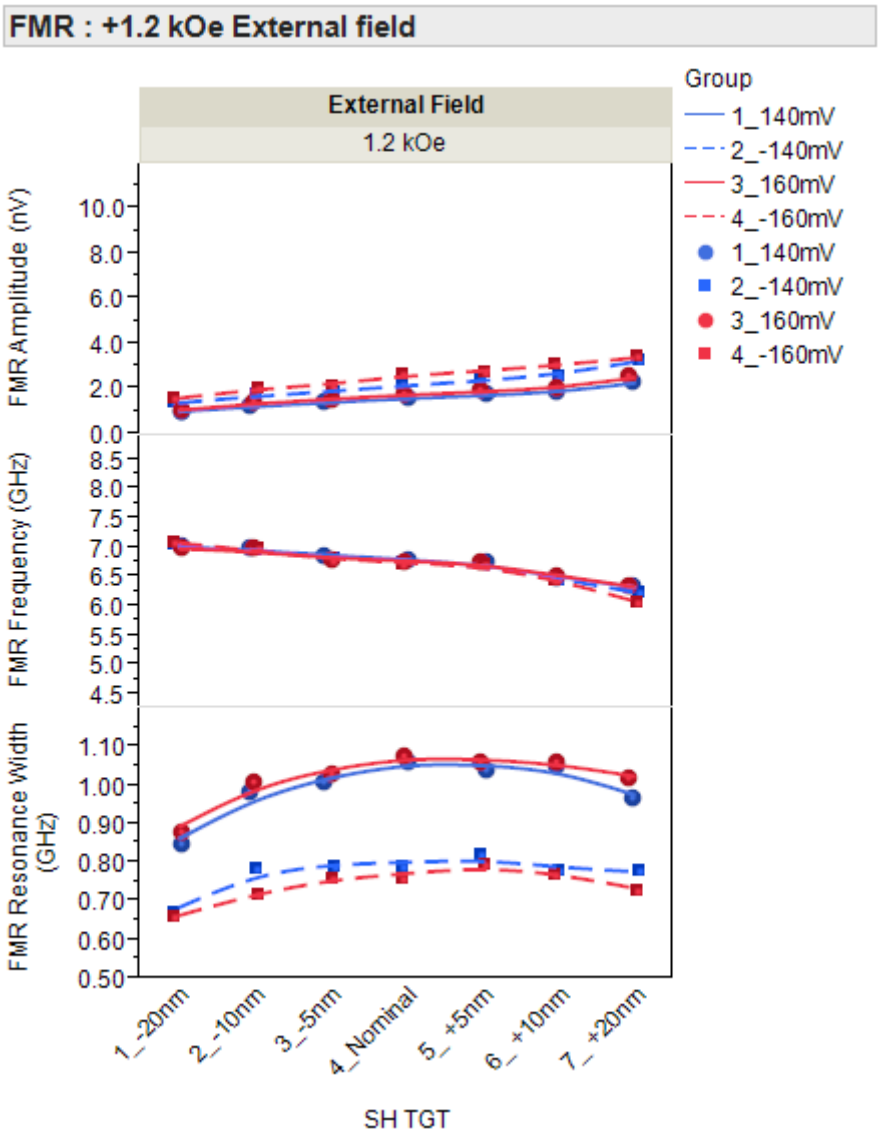

Fig. 4.18 FMR spectrum trend of magnetic read sensor with various SH targets with +1.2 kOe applying external magnetic field

However, the other new finding on this condition applying +1.2 kOe external magnetic fields was a secondary FMR peak in high frequency happened at the longer SH. The secondary FMR peak occurred at the long SH scales since +10nm and +20nm SH from nominal which they showed the same trend for all set up of volt biases. The detailed analysis suggests that some layer of magnetic read sensor has been abnormal behavior suspected from permanent magnet material. As permanent magnet design used in the experiment was the soft bias material which had magnetic property similar to free layer material. Therefore, permanent magnet can be weaken magnetization at the longer SH under applying high external magnetic field in longitudinal direction which results to generate secondary FMR peak close to majority FMR peak of free layer.

The works in [10], [11], [14] and [21] have been reported on additional FMR peak under applying high external magnetic field in transverse direction explained by considering the result of magnetization fluctuation on reference/pinned layer. This condition supposes that magnetization of free layer is nearly antiparallel to reference layer. However, those previous works have applied high external magnetic field in transverse direction to permanent magnet which is different direction from this experiment applying in longitudinal direction. As a result, the additional FMR peak can be generated from magnetization motion of all layers of magnetic read sensor which depends on the level and direction of applying external magnetic field.

In term of heat effect, forward volt bias with +160mV showed comparable FMR spectrum composed of FMR amplitude, FMR frequency and FMR resonance width compared to +140mV volt bias. The FMR spectrum with +160mV volt bias on the shortest and longest SH target under applying +1.2kOe external field are shown in Fig. 4.16 (a) and (b), respectively. All SH scales displayed the same comparison of FMR spectrum between +160mV and +140mV volt bias as shown in Fig. 4.18. The reverse volt bias, -160mV also showed comparable FMR spectrum compared to -140mV volt bias. This result was the same trend as the comparison between two levels of forward volt biases under applying +1.2 kOe external magnetic fields as shown in Fig. 4.18. The FMR spectrum with -140mV and -160mV volt bias on the shortest and longest SH with applied +1.2 kOe external magnetic field are shown in Fig. 4.15 and Fig. 4.17, respectively. All SH scales showed the same trend of FMR comparison between two levels of volt bias. Hence, the level of volt bias has not effected on FMR spectrum under applying +1.2 kOe external magnetic field.

At the same level of volt bias, the +140mV forward volt bias showed slightly lower FMR amplitude but significantly higher FMR resonance width compared to -140mV reverse volt bias as illustrated in Fig. 4.18. While FMR frequency was comparable between opposite direction of volt bias. The comparison of FMR behavior between +160mV and -160mV volt bias was the same trend as +140mV and -140mV volt bias. It is likely that forward volt bias has presented better switching time of magnetic read sensor due to higher damping. These results have been detected by higher FMR resonance width as referred in Equation 2.24 which is the same trend as condition of applying no external magnetic field. Interestingly, FMR spectrum can detect the direction of volt bias by parameter of FMR resonance width while the level of volt bias has no impact on FMR behavior during applying +1.2 kOe external magnetic fields.

Next section, magnetic read sensor with varied SH scales were performed on FMRA with -1.2 kOe applying external magnetic field in longitudinal direction to permanent magnet. The volt biases were applied both forward and reverse directions with different levels as condition of +1.2 kOe and 0 Oe applying external magnetic field. Figure 4.19 shows the FMR spectrum on magnetic read sensor of two different SH targets with -1.2 kOe applying external magnetic field and +140 mV volt bias. The shortest SH target (-20nm SH from nominal) is shown in Fig. 4.19 (a). The longest SH target (+20nm SH from nominal) is illustrated in Fig. 4.19 (b). For the shortest SH, FMR amplitude was 1.46 nV, FMR frequency was 6.94 GHz and FMR resonance width was 0.71 GHz. For the longest SH, FMR amplitude was slightly increased to 2.05 nV, FMR frequency was slightly shifted up to 7.26 GHz and FMR resonance width was slightly wider to 0.81 GHz. FMR amplitude, frequency and resonance width demonstrated slightly difference between shortest and longest SH. The longest SH, a secondary FMR peak in high frequency was found as shown in Fig. 4.19 (b). The other set up of volt biases composed of -140mV, +160mV and -160mV volt bias also found the secondary FMR peak in high frequency at the longest SH as shown in Fig. 4.20 (b), Fig. 4.21 (b) and Fig. 4.22 (b), respectively. These FMR comparisons between shortest and longest showed the same result as condition of +1.2 kOe applying external magnetic field. There were slightly changing of FMR spectrum between shortest and longest SH and found the secondary FMR peak in high frequency at the longest SH on both condition of +1.2 kOe and -1.2 kOe applying external field.

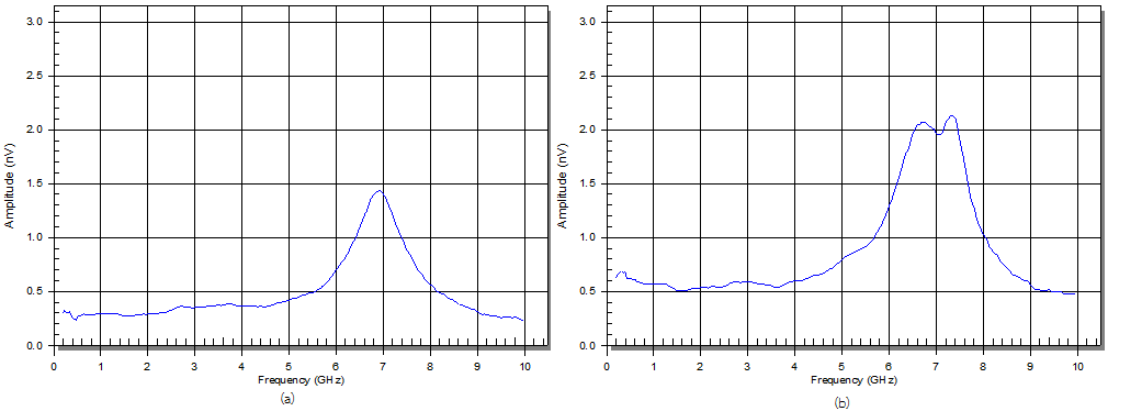

Fig. 4.19 FMR spectrum with applying -1.2 kOe external magnetic field with +140 mV volt bias for two different SH targets of TMR sensor (a) shortest SH target is -20nm SH from nominal (b) longest SH target is +20nm SH from nominal

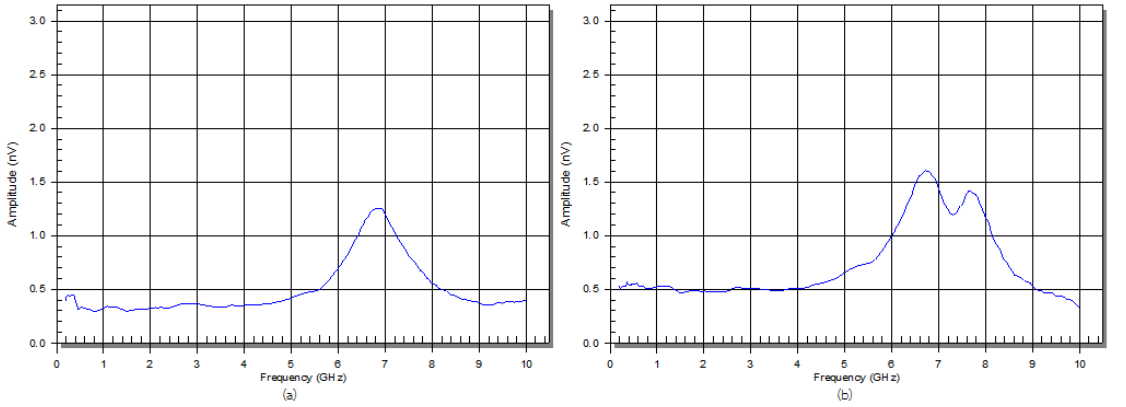

Fig. 4.20 FMR spectrum with applying -1.2 kOe external magnetic field with -140 mV volt bias for two different SH targets of TMR sensor (a) shortest SH target is -20nm SH from nominal (b) longest SH target is +20nm SH from nominal

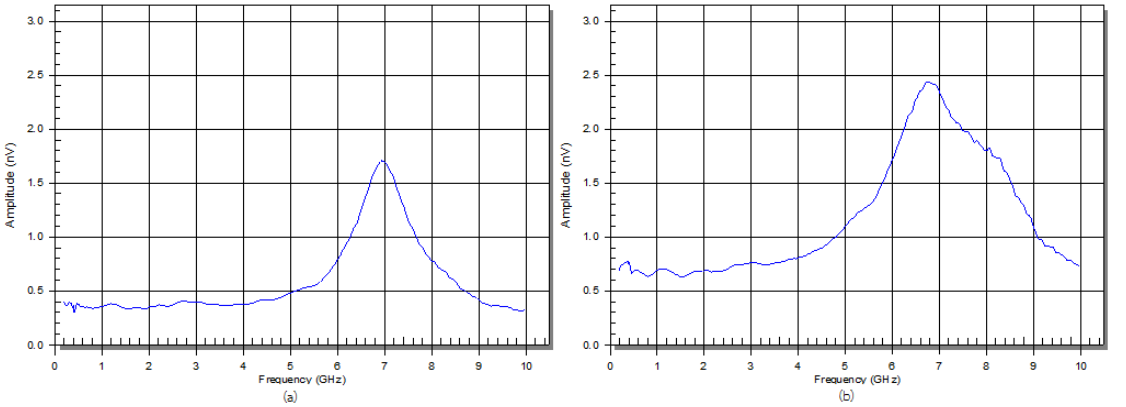

Fig. 4.21 FMR spectrum with applying -1.2 kOe external magnetic field with +160 mV volt bias for two different SH targets of TMR sensor (a) shortest SH target is -20nm SH from nominal (b) longest SH target is +20nm SH from nominal

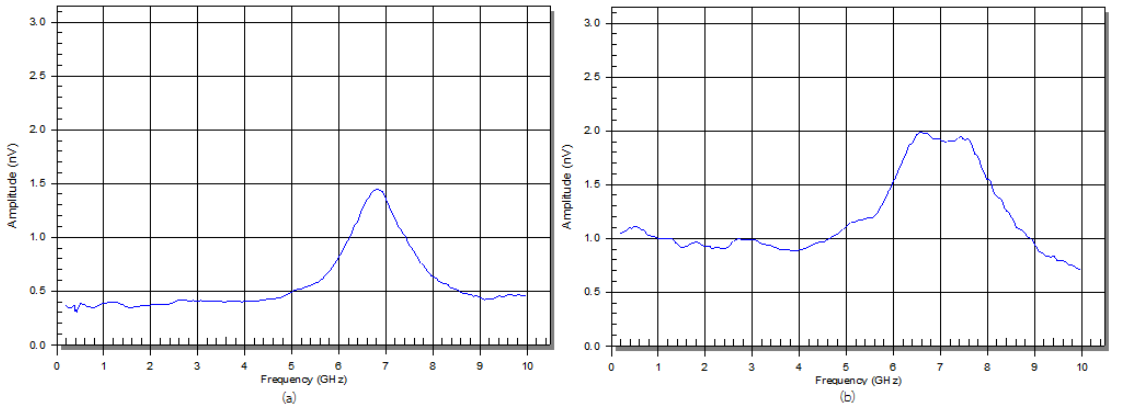

Fig. 4.22 FMR spectrum with applying -1.2 kOe external magnetic field with -160 mV volt bias for two different SH targets of TMR sensor (a) shortest SH target is -20nm SH from nominal (b) longest SH target is +20nm SH from nominal

Table 4.4 shows the summary of FMR result for magnetic read sensor between seven SH targets (-20nm, -10nm, -5nm, nominal, +5nm, +10nm, +20nm) with -1.2 kOe applying external magnetic field in longitudinal direction and varied set up of volt biases. The results displayed slightly decreased FMR amplitude and FMR resonance width as the SH was shorter. In term of FMR frequency was comparable for all SH scales. These finding were plotted in Fig. 4.23 referred to FMR data in Table 4.4. The results appear that the behavior of FMR spectrum did not depend on SH scale which was the same as condition of +1.2 kOe applying external magnetic field.

Table 4.4 Summary of the FMR result for magnetic read sensor with seven SH targets from -20nm SH to +20nm SH target with -1.2 kOe applying external magnetic field

External field	-1.2 kOe							
Parameter		SH TGT						
	Volt Bias	-20nm	-10nm	-5nm	Nominal	+5nm	+10nm	+20nm
FMR Amplitude (nV)	140mV	1.46	1.81	1.88	1.88	1.93	1.87	2.05
	-140mV	1.25	1.43	1.56	1.64	1.68	1.57	1.73
	160mV	1.71	2.08	2.17	2.18	2.32	2.16	2.37
	-160mV	1.42	1.70	1.76	1.85	1.90	1.76	1.95
FMR Frequency (GHz)	140mV	6.94	6.91	6.90	7.12	7.04	7.02	7.26
	-140mV	6.82	6.84	6.84	6.93	6.89	6.89	6.65
	160mV	6.96	6.92	6.94	7.06	7.03	6.96	6.89
	-160mV	6.83	6.82	6.86	6.97	6.87	6.86	6.55
FMR Resonance Width (GHz)	140mV	0.71	0.80	0.83	0.88	0.96	0.91	0.81
	-140mV	0.87	0.99	1.00	1.13	1.16	1.07	0.97
	160mV	0.69	0.79	0.84	0.93	0.96	0.91	0.84
	-160mV	0.86	1.00	1.03	1.09	1.17	1.08	0.96

All set up of volt biases composed of +140mV, -140mV, +160mV and -160mV demonstrated the same trend of FMR spectrum in varied SH scales that showed slightly changing of FMR amplitude, FMR frequency and FMR resonance width as the SH was shorter. These slightly changing of the FMR spectrum in various SH scales were similar to condition of +1.2 kOe external magnetic field which the external magnetic field driven the free layer to the magnetization saturation [14] and [21]. In addition, all set up of volt biases were found secondary FMR peak in high frequency at the longer SH. This additional FMR peak was the result of weaken magnetization of permanent magnet as previous detailed analysis in condition of applying +1.2 kOe external magnetic fields.

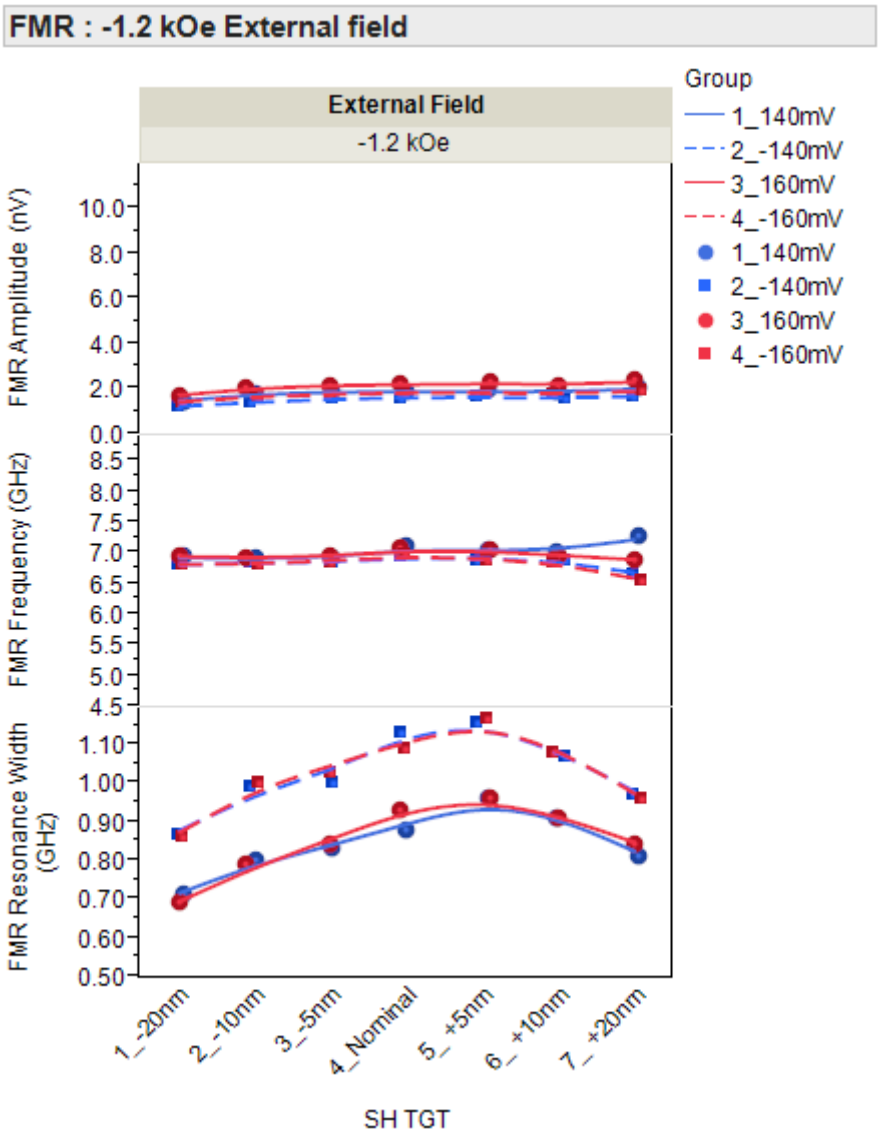

Fig. 4.23 FMR spectrum trend of magnetic read sensor with various SH targets with -1.2 kOe applying external magnetic field

In term of heat effect, forward volt bias with +160mV showed comparable FMR spectrum compare to +140mV volt bias that was the same trend for all SH scales as displayed in Fig. 4.23. The FMR spectrum with +160mV volt bias on the shortest and longest SH targets under applying -1.2kOe external field are shown in Fig. 4.21 (a) and (b), respectively. The reverse volt bias, -160mV volt bias also demonstrated comparable FMR spectrum compared to -140mV volt bias. This result was the same trend as the comparison between two levels of forward volt bias under applying -1.2 kOe external magnetic fields as shown in Fig. 4.23. The FMR spectrum with -140mV and -160mV volt bias on the shortest and longest SH with applied -1.2 kOe external magnetic field are shown in Fig. 4.20 and Fig. 4.22, respectively. Therefore, the level

of volt bias has had no impact on FMR spectrum under applying -1.2 kOe and +1.2 kOe external magnetic fields.

At the same level of volt bias, the +140mV forward volt bias showed slightly higher FMR amplitude but significantly lower FMR resonance width compared to -140mV reverse volt bias as illustrated in Fig. 4.23. The FMR frequency was comparable between opposite direction of volt bias. The comparison of FMR behavior between +160mV and -160mV volt bias was the same trend as comparison between +140mV and -140mV volt bias under applying -1.2 kOe external magnetic fields. It is likely that forward volt bias has not presented better switching time of magnetic read sensor as condition of 0 Oe and +1.2k Oe applying external magnetic field. The results can be explained by lower damping due to lower FMR resonance width on forward volt bias as referred in equation 2.24. This trend of FMR resonance width has been opposite trend to previous conditions of applying external magnetic fields as shown in Fig. 4.24. Figure 4.24 presents the overall FMR spectrum trend of magnetic read sensor with various SH targets and applying 0 Oe, +1.2 kOe and -1.2 kOe longitudinal external magnetic fields with varied volt biases both level and direction. However, the direction of volt bias can be detected by FMR resonance width that depends on condition of applying external magnetic field.

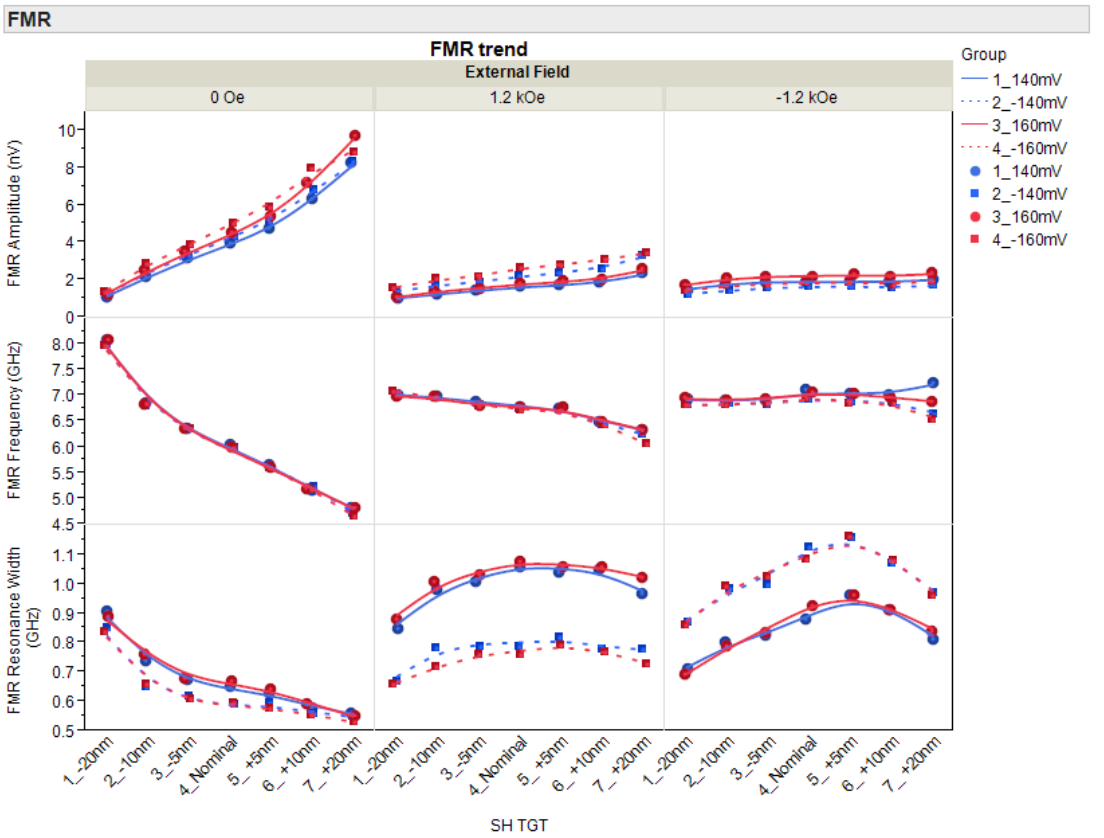

Fig. 4.24 Overall FMR spectrum trend with applying external magnetic field in longitudinal direction on magnetic read sensor with various SH targets

Under applying no external magnetic field, FMR spectrum which depends on SH scale is generated from magnetization fluctuation of free layer. The study suggest that the SH scale plays some roles on the effective stiffness field of free layer due to change of shape anisotropy. QST result has corresponded to effective stiffness field trend in various SH scales that has shown less sensitivity and SNR as the SH is shorter. Once the high external magnetic fields have been applied in longitudinal direction both +1.2 kOe and -1.2 kOe, FMR spectrum has been slightly changed on various SH scales caused by external magnetic field driven the magnetization of free layer into saturation state. At the longer SH a secondary FMR peak in high frequency is found, it has been generated by weaken magnetization of permanent magnet. This study is found that the effect of heat has indicated by FMR amplitude parameter which can be displayed only the condition of applying no external magnetic field. Interestingly, FMR spectrum can detect the direction of volt bias by parameter of FMR resonance width. It appears that forward volt bias with 0 Oe and +1.2 kOe applying longitudinal magnetic field have better switching time of magnetization than reverse volt bias. These results have based on higher damping due to higher FMR resonance width parameters. In term of -1.2 kOe applying external magnetic field, the switching time of magnetic read sensor has shown worse on forward volt bias which is opposite trend to previous condition of the experiment. These results seems that direction of volt bias have an impact on switching time of magnetization of magnetic read sensor.

4.4 Transverse field dependence of the FMR spectrum

The last section was the study of symmetry of magnetic read sensor as various SH scales with applying external magnetic field in transverse direction to permanent magnet. The transverse field was applied with the same level but opposite polarity composed of +520 Oe and -520 Oe. The experiments were conducted with two levels of volt bias in forward and reverse directions which were the same set up as previous conditions. The volt biases were composed of 140mV and 160mV. Ideally, symmetry of magnetic read sensor, positive and negative polarity is given the same sensitivity and signal. However, the asymmetry still occurs as the magnetic read sensor keep shrinking the dimensions and changing the new reader design to support higher areal density that is very important to study on this behavior.

Figure 4.25 shows the FMR spectrum of magnetic read senor on the shortest and longest SH with applying transverse field in opposite polarities composed of +520 Oe and -520 Oe and +140 mV volt bias. For the shortest SH with -520 Oe transverse fields, FMR amplitude was about 1.2 nV and FMR frequency was 8.1 GHz as shown in Fig. 4.25 (a). At +520 Oe transverse fields, FMR amplitude was about 1.0 nV and FMR

frequency was 8.2 GHz which showed similar FMR spectrum to -520 Oe transverse fields. The shortest SH as illustrated in Fig. 4.25 (a) demonstrated the superposition of two FMR spectrums for symmetrical magnetic read sensor. The longest SH, FMR peaks were shifted between different polarities transverse field as shown in Fig. 4.25 (b). For -520 Oe transverse fields, FMR amplitude was about 5.9 nV and FMR frequency was about 5.4 GHz. For opposite polarity transverse field which was +520 Oe, FMR amplitude was increased to 7.1 nV and FMR frequency was shifted down to 4.9 GHz. The shortest SH of magnetic read sensor showed lower delta of FMR amplitude, FMR frequency and FMR resonance width in applying transverse magnetic fields compared to longest SH.

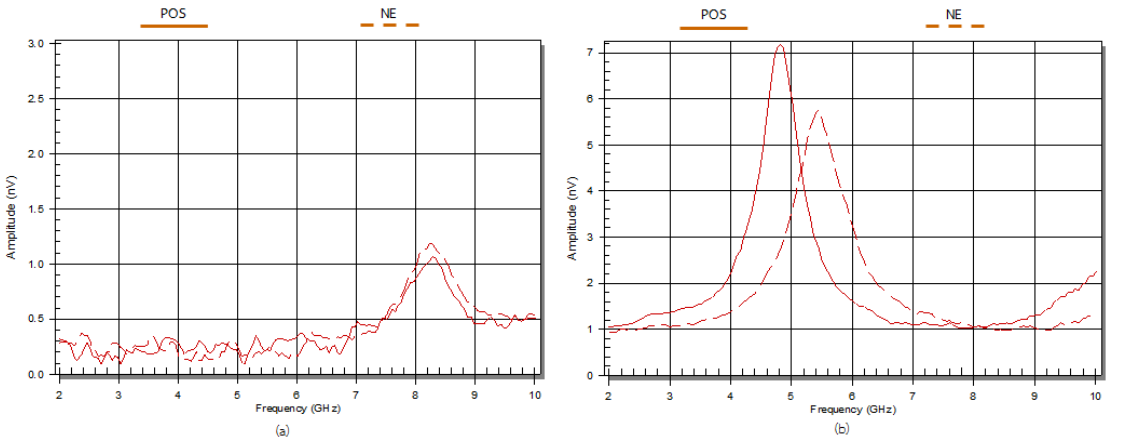

Fig. 4.25 FMR spectrum with applying +520 Oe and -520 Oe transverse field with +140 mV volt bias for two SH targets of TMR sensor (a) shortest SH target is -20nm SH from nominal (b) longest SH target is +20nm SH from nominal

It appears that the symmetry of magnetic read sensor has considered by the delta of FMR amplitude and FMR frequency between opposite polarities of transverse magnetic fields. Hence, the shortest SH of magnetic read sensor has exhibited more symmetrical magnetic read sensor than the longer one since the shorter SH shows less delta FMR spectrum in transverse magnetic fields of opposite polarities. The other set up of volt biases composed of -140mV, +160mV and -160mV also found that the shortest SH performed less delta FMR spectrum between opposite polarities of transverse magnetic field compared to longest SH as shown in Fig. 4.26, Fig. 4.27 and Fig. 4.28, respectively. These results suggest that magnetic read sensor has displayed more symmetrical at the shortest SH.

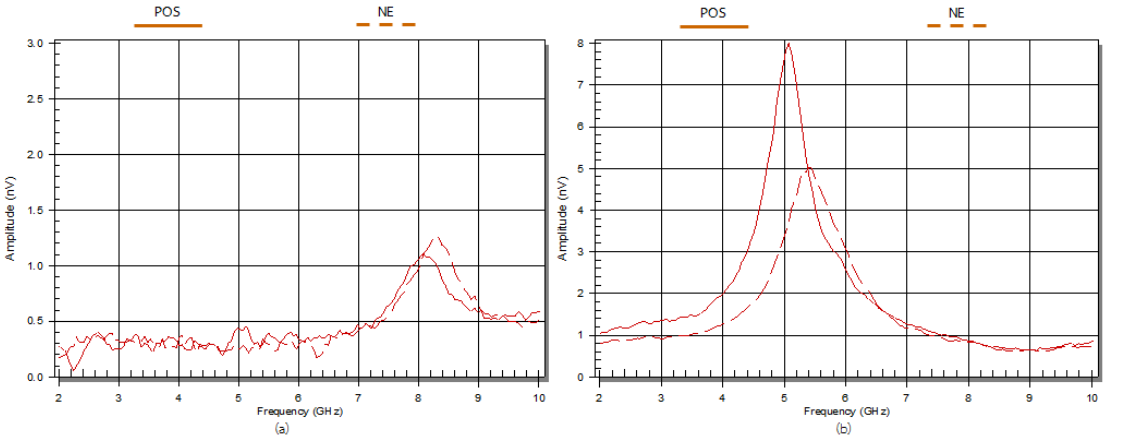

Fig. 4.26 FMR spectrum with applying +520 Oe and -520 Oe transverse field with -140 mV volt bias for two SH targets of TMR sensor (a) shortest SH target is -20nm SH from nominal (b) longest SH target is +20nm SH from nominal

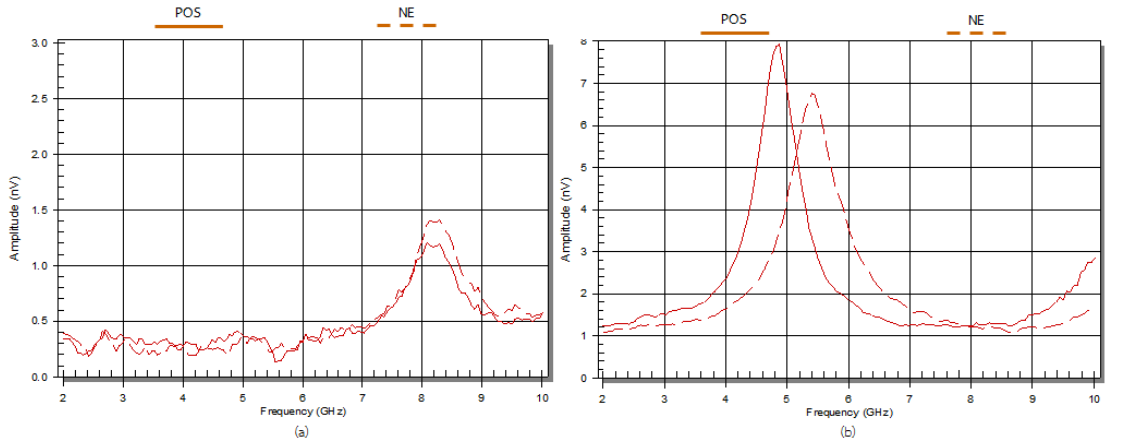

Fig. 4.27 FMR spectrum with applying +520 Oe and -520 Oe transverse field with +160 mV volt bias for two SH targets of TMR sensor (a) shortest SH target is -20nm SH from nominal (b) longest SH target is +20nm SH from nominal

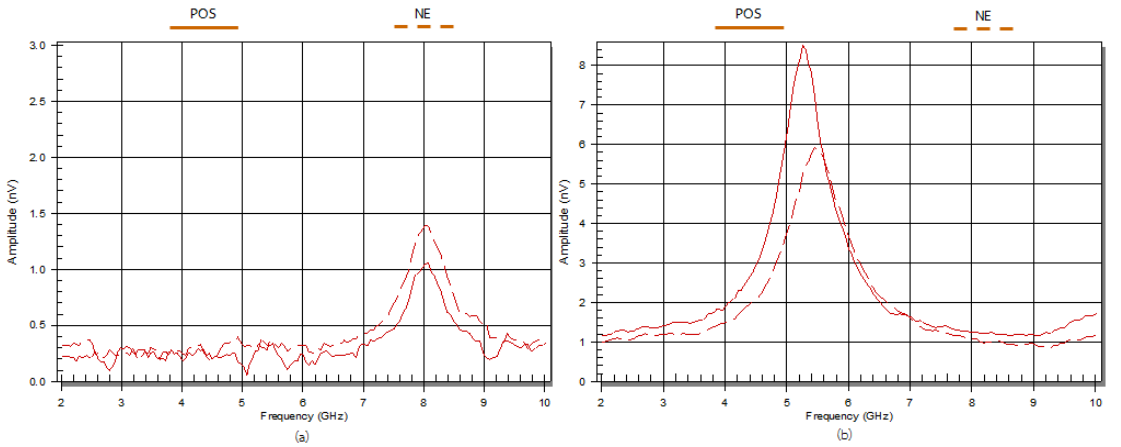

Fig. 4.28 FMR spectrum with applying +520 Oe and -520 Oe transverse field with -160 mV volt bias for two SH targets of TMR sensor (a) shortest SH target is -20nm SH from nominal (b) longest SH target is +20nm SH from nominal

Table 4.5 shows the summary of delta FMR spectrum for magnetic read sensor between seven SH targets applying with opposite polarities of transverse magnetic field and varied set up of volt biases. The result showed less delta FMR amplitude, FMR frequency and FMR resonance width as the SH was shorter. The delta FMR spectrum also closed to zero at the shorter SH. These finding were plotted in Fig. 4.29 referred to Table 4.5 that showed the trend of delta FMR spectrum in transverse magnetic fields of opposite polarities. All set up of volt biases composed of +140mV, -140mV, +160mV and -160mV exhibited the same trend of delta FMR spectrum in various SH scales.

Table 4.5 Summary of the delta FMR between with +520Oe and -520 Oe applying external magnetic field in transverse direction for magnetic read sensor with seven SH targets from -20nm SH to +20nm SH target

	Group	SH TGT						
		-20nm	-10nm	-5nm	Nominal	+5nm	+10nm	+20nm
Delta FMR Amplitude	140mV	-0.20	-0.30	-0.40	-0.40	-0.40	-0.10	0.30
	-140mV	0.00	0.10	-0.10	0.50	0.50	1.15	2.20
	160mV	-0.20	-0.30	-0.60	-0.50	-0.70	-0.15	0.10
	-160mV	0.00	0.10	-0.10	0.55	0.70	1.25	2.00
Delta FMR Frequency	140mV	-0.10	0.00	0.10	-0.10	-0.10	-0.20	-0.40
	-140mV	-0.10	0.00	0.10	-0.10	-0.05	-0.10	-0.30
	160mV	-0.10	0.00	0.10	-0.10	0.00	-0.10	-0.30
	-160mV	-0.10	0.00	0.10	-0.10	0.00	-0.10	-0.30
Delta FMR Resonance Width	140mV	0.00	0.10	0.10	0.00	0.00	0.00	0.00
	-140mV	-0.10	-0.10	0.00	-0.10	-0.10	-0.10	-0.20
	160mV	0.05	0.10	0.10	0.10	0.10	0.05	0.00
	-160mV	-0.10	-0.10	-0.05	-0.10	-0.10	-0.10	-0.10

This study appears that the delta FMR spectrum has depended on SH scale. The result has shown better symmetrical magnetic read sensor as the SH is shorter. The shifts of FMR spectrum in transverse field of opposite polarities are translated into different sensitivity of the read sensor for positive and negative transition. The study suggests that overlapping has been better than underlapping because it is more symmetry at the shorter SH. FMR data can provide the finer limitation of SH for lapping process in narrower range than that of QST. The SH limit by FMRA has demonstrated that it should not be over +10nm from nominal as shown in Fig. 4.29 while QST data has given the limit at +20nm from nominal as illustrated in Fig. 4.7. These results imply that FMR data is able to identify the finer scale of SH for lapping process which can be used for screening bad magnetic material from production. In term of heat effect, the forward volt bias with +160mV showed comparable delta

FMR spectrum compared to +140mV volt bias that was the same trend for all SH scales as illustrated in Fig. 4.29. The reverse volt bias, -160mV volt bias also demonstrated comparable delta FMR spectrum to -140mV volt for all SH scales. This result was the same trend as comparison between two levels of forward volt bias as shown in Fig. 4.29. The study suggests that the effect of heat has had no influence on symmetrical magnetic read sensor since it shows comparable delta FMR spectrum between two levels of volt bias. The direction of volt bias can be significantly detected by delta FMR resonance width that is opposite trend between forward and reverse direction. These results suggest that the direction of volt bias have had an impact on switching time of magnetic read sensor detected by its damping from behavior of FMR resonance width as studied in [24] and [25].

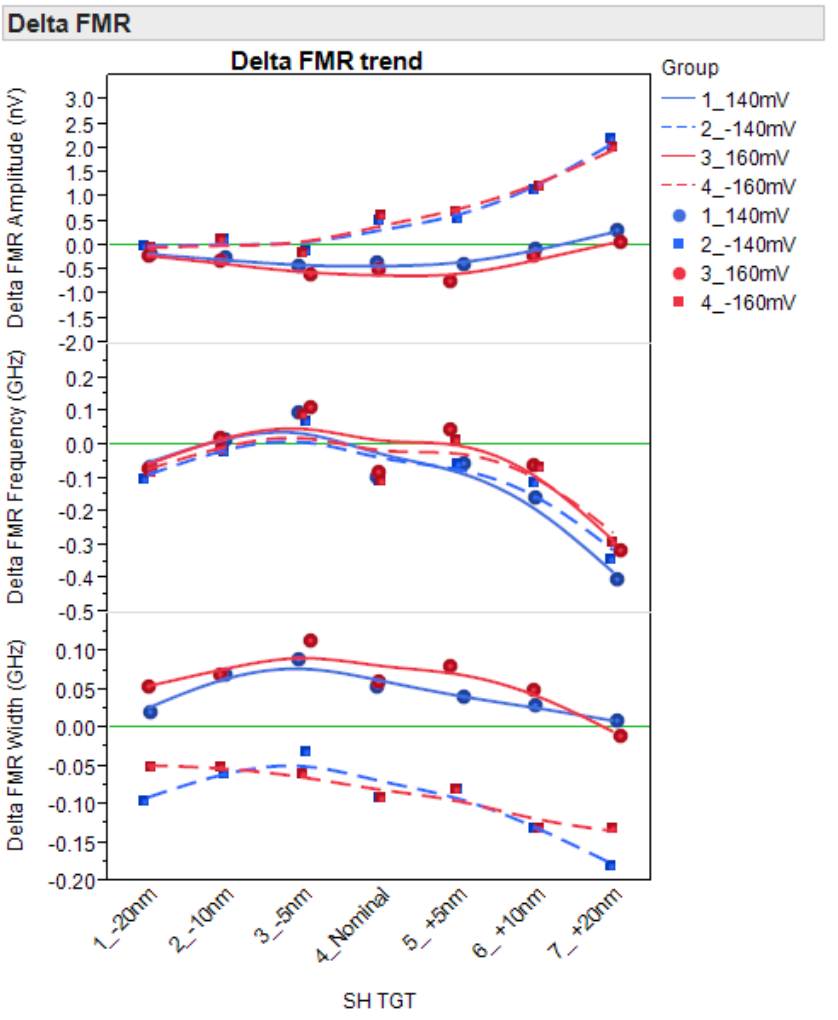

Fig. 4.29 The trend of delta FMR spectrum with applying opposite polarity transverse field (+520 Oe and -520 Oe) on magnetic read sensor with various SH targets

Chapter 5
Conclusions and suggestions

This research is to study the characterization of Tunneling Magneto Resistive (TMR) read sensor with multiple Stripe Height (SH) by using ferromagnetic resonance analyzer (FMRA) in comparison to quasi-static test (QST). TMR heads with various SH scales were performed on FMRA composed of varied external magnetic fields and set up of volt biases. Under no external magnetic field condition, the FMR spectrum in various SH scales are generated by magnetization fluctuation of free layer. The results have shown increased effective stiffness field as the SH is shorter. This can be observed through the trend of increasing in FMR frequency and decreasing in FMR amplitude. It is found that the behavior of FMR spectrum has depended on SH scales which have related to the effective stiffness field due to change of shape anisotropy. These results suggest that SH scale plays some roles on the effective stiffness field of free layer which has an effect on read ability of magnetic read sensor. QST results have corresponded to the effective stiffness field trend that has presented less sensitivity and lower signal to noise ratio at the shorter SH. These finding imply that QST amplitude and SNR are inversely related to parameter of FMR frequency. It would be interesting to estimate some important QST parameters of magnetic read sensor by using the FMR measurement that is able to enhance its detection capabilities for magnetic recording industry.

Once the high external magnetic fields are applied in longitudinal direction, FMR spectrum has been slightly changed on various SH scales caused by external magnetic driven the magnetization of free layer into saturation state [14] and [21]. For the longer SH a secondary FMR peak in high frequency has been found. The detailed analyses suggest that this additional FMR peak has been the result of weaken magnetization of permanent magnet. The works in [10], [11], [14] and [21] have been reported on additional FMR peak under applying high external magnetic field in transverse direction explained by considering the result of magnetization fluctuation on reference/pinned layer. This condition has supposed that magnetization of free layer is nearly antiparallel to reference layer. However, those previous works have been applied high external magnetic field in transverse direction to permanent magnet which is different direction from this experiment applying in longitudinal direction. Therefore, the additional FMR peak can be generated from any layer of magnetic read sensor which depends on the level and direction of applying external magnetic field. In term of symmetrical characteristic of magnetic read sensor, it has shown less delta FMR spectrum in transverse magnetic field of

opposite polarities as the SH is shorter. The shifts of FMR spectrum in transverse magnetic field of opposite polarities are translated into different sensitivity of the sensor for positive and negative transition. The study seems that the delta FMR spectrum has depended on SH scale which has shown better symmetrical magnetic read sensor as the SH is shorter. These finding suggest that overlapping has been better than underlapping because it is more symmetry at the shorter SH. It is found that QST has been able to exhibit the heat effect while FMR data has displayed slightly difference FMR behavior between two levels of volt biases. Interestingly; FMRA can detect the direction of bias voltage from parameter of FMR resonance width that closely relates to the damping. The experiments demonstrate that forward volt bias has performed better switching time of magnetization than reverse volt bias detected by higher damping from parameter of FMR resonance width as suggested in [24] and [25]. It is unlikely that QST results have not been able to detect direction of volt bias.

FMRA is able to provide the characteristic of magnetic read sensor composed of magnetic property and more detailed than QST composed of electrical property. However, FMRA has low unit per hour (UPH) than QST which is able to test the sample in special case with small quantity. Nevertheless, it is very interesting to carry on the further study of new design of magnetic read sensor with varied SH scales by using FMRA and applying external magnetic field both transverse and longitudinal direction in order to understand all magnetic property by layer-level state. FMR information can provide the finer limitation of SH for lapping process in a narrower range than that of QST. The SH limit by FMRA has shown that it should not be over +10nm from nominal while QST data has indicated the limit at +20nm from nominal. These results imply that FMR data is able to identify the finer scale of SH for lapping process which can be used for screening bad magnetic material and unstable sensor from production. The cost reduction is gained for less drive failure by providing information for lapping process with finer range of lapping. Per experiment data, FMR parameters have strong correlation to QST parameters. Therefore, industry can project and predict spec for screening magnetic properties at QST tester in additional to electrical properties screening. By using this method, it will enhance the quality and efficiency in testing of magnetic reader sensor performance more accurately and more precisely.

Reference

[1] Ed Grochowski, **"The Hard Disk Drive: A Mature, Important Storage Technology"**,http://www.storageacceleration.com/author.asp?section_id=3670&doc_id=274482, Aug.2014.

[2] S. Kamwan, W. Pijitrojana and C. Sa-ngiamsak, **"Effect of Track Width and Stripe Height Ratio on the Characteristics of CPP-GMR and TMR heads",** IEEE Trans. Magn., vol. 24, no.12, Oct.2011.

[3] J. Matsugi, Y. Mizoh and T. Nakano, **"ESD Phenomena in GMR heads in the Manufacturing Process of HDD and GMR Heads",** IEEE Trans. Magn. vol. 28, no. 3, Jul.2005.

[4] A. Taratorin, **"Measurement of Effective Free Layer Magnetization Orientation of TMR Sensors",** IEEE Trans. Magn., vol. 45, no. 10, Oct.2009.

[5] S. Mao *et al*., **"Tunneling Magnetoresistive Heads Beyond 150 Gb/in^2",** IEEE Trans. Magn., vol. 40, no. 1, Jan.2004.

[6] S. Mao *et al*., **"Commercial TMR Heads for Hard Disk Drives: Characterization and Extendibility At 300 Gbit/in^2",** IEEE Trans. Magn., vol. 42, no. 2, Feb.2006.

[7] G. C. Han, E. L. Tan, B. Y. Zong, Y. K. Zheng, S. G. Tan, and L. Wang, **"Abnormal Increase in Ferromagnetic Resonance Amplitude just before the Breakdown in Tunnel Magnetoressitive Head",** J. Appl. Phys., vol. 103, Feb.2008.

[8] Denny D. Tang and Y. Jen Lee. **"Magnetic Memory Fundamental and Technology",** UK: Cambridge University Press, Inc2010.

[9] J. R. Childress, R. E. Fontana Jr., **"Magnetic Recording Read Head Sensor Technology",** C. R. Physique., vol 6, 2005.

[10] J. Masuko, H. Akimoto, M. Matsumoto, H. Kanai and Y. Uehara, **"Amplitude and Phase Distributions of Magnetization in Tunneling Magnetoresistive Heads"**, IEEE Trans. Magn. vol. 44, no. 7, Jul.2008.

[11] J. C. Jury, Student member; IEEE, K. B. Klaassen, J C. L. van Peppen, S. X. Wang and member; IEEE, **"Measurement and Analysis of Noise Sources in Giant Magnetoresistive Sensors up to 6 GHz",** IEEE Trans. Magn., vol. 38, no. 5, Sep.2002.

[12] MRS200 Operation Manual, **"Quasistatic Slider-Level Tester"**, Operation Manual, Dec.2000.

[13] Y. Chen, D. Song and J Qiu *et al*.,**"2Tbit/in^2 Reader Design Outlook"**, IEEE Trans. Magn. vol. 46, no.3, Mar.2010.

[14] G. C. Han., B. Y. Zong, P. Luo, L Wang and S. N. Mao, **"Hard Bias Effect on Magnetic Noise in Different Types of Tunnel Magnetoresistive Heads",** IEEE Trans. Magn. vol.44, no.11, Nov.2008.

[15] K. B. Klaassen, J. van Peppen, and X. Xing, **"Simulation of Noise, Signal-to-Noise and Bandwidth of TMR and CIP/CPP GMR heads",** IEEE Trans. Magn. vol. 42, no.2, Feb.2006.

[16] T. L. Gilbert, **"A Phenomenological Theory of Damping in Ferromagnetic Material",** IEEE Trans. Magn. Vol. 40, no.6, Nov.2004.

[17] K. B. Klaassen, Fellow, IEEE, X. Xing and J. van Peppen, **"Broad-band Noise Spectroscopy of Giant Magnetoresistive Read Heads",** IEEE Trans. Magn. Vol.42, no.7, Jul.2005.

[18] Jian-Gang Zhu, **"Thermal Magnetic Noise and Spectra in Spin Valve Heads",** J.Appl. Phys., vol. 91, no.10, May.2002.

[19] Y. Zhou, J. Zhu and N. Kim, **"Thermally Excited Ferromagnetic Resonance as Diagnostic Tool for Spin Valve Heads",** J.Appl. Phys., vol. 93, no.10, May.2003.

[20] O. Heinonen and H. Cho., **"Thermal Magnetic Noise in Tunneling Readers",** IEEE Trans. Magn. Vol.40, no.4, Jul.2004.

[21] G. C. Han, Y. K. Zheng, Z. Y. Liu and B.Liu, **"Field Dependence of High Frequency Magnetic Noise in Tunneling Magneto Resistive Heads",** J. Appl. Phys., vol.100, Sep.2006.

[22] Y.Endo, T. Abe and M. Yamaguchi, **"Spin-Torque Effect on Thermally Excited Magnetization Fluctuation Noise in Tunneling Magnetoresistive Read Heads",** IEEE Trans. Magn. vol. 47, no. 10, Oct.2011.

[23] W. Kuch, **"Ferromagnetic Resonance (FMR)"**, Fachbereich Physik, http://www.physik.fuberlin.de/einrichtungen/ag/agkuch/research/techniques/fmr/index.html.

[24] Stuart S. P. Parkin et al., **"Magnetic Domain-wall Racetrack Memory"**, Science. Magn. vol. 320, Apr.2008.

[25] Myers, E. B. et al., **"Nature Material"**, Magn. vol.11, May.2012.

APPENDICES

Appendix A
Conference proceeding

Electrical Engineering Academic Association (Thailand) The 2015 International Electrical Engineering Congress

The 2015 International Electrical Engineering Congress

(*i*EECON2015)

This certificate is presented to

PRAPINPORN WEAWHONGSE

For recognition of presenting a paper in the conference

Characterization of Tunneling Magneto Resistive (TMR) Head with Multi-Stripe height by using Ferro Magnetic Resonance Analyzer (FMRA)

During March 18-20, 2015, Phuket City, Thailand

Professor Dr. Apirat Siritaratiwat

*i*EECON2015 General Chair

Applied Mechanics and Materials Vol 781 (2015) pp 195-198
© (2015) Trans Tech Publications, Switzerland
doi:10.4028/www.scientific.net/AMM.781.195

Submitted: 2014-10-13
Revised: 2015-03-30
Accepted: 2015-04-06

Free layer Characterization of TMR head with multi-stripe height by using Ferro Magnetic Resonance Analyzer (FMRA)

P. Weawhongse[1, a *], C.Sa-ngiamsak [2,b], W. Pijitrojana[3,c], K.Vichienchom[4,d]

College of Data Storage Innovation

King Mongkut's Institute of Technology Ladkrabang

Ladkrabang, Bangkok 10520, Thailand

[a]Prapinporn.w@gmail.com, [b]c.sangiamsak@gmail.com, [c]pwanchai@engr.tu.ac.th, [d]kvkasin@gmail.com

Keywords: Ferromagnetic resonance analyzer (FMRA), Tunneling Magneto Resistive head (TMR), Stripe height (SH), free layer, reference layer and stiffness field

Abstract. As continued reducing the track width (TW) of magnetic read sensor for gaining areal density in hard disk drive (HDD) industry, stripe height (SH) is needed to be reduced as keeping aspect ratio(TW/SH) for maintain resistance and signal constant. This paper is proposed to characterize the free layer behavior of tunneling magneto resistive (TMR) head with multiple SH by using ferro magnetic resonance analyzer (FMRA) that is able to analyze by layer-level state without applying external field. The results are found that, at shorter SH, effective stiffness field of free layer is increased which is based on decreasing FMR amplitude and increasing FMR frequency. As a result, magnetic read sensor is shown less sensitivity and signal to noise ratio (SNR) with shorter SH. The SH is a correlated function of the effective stiffness field in free layer that is referred to changed shape anisotropy field which has an effect to read ability.

Introduction

According to continued increase of areal density in magnetic recording, the dimension of magnetic read and write sensor are continued decreasing with complex designs. Presently, magnetic read sensor is based on Tunneling Magneto Resistance (TMR) technology that is able to improve the read ability and reliability as shrinking size.

Stripe height (SH) is a key physical dimension which is a length of magnetic read sensor [5] and is controlled by lapping process of slider fabrication. The SH is proportional to the volume of magnetic read sensor that is significantly impact to head sensitivity. As continued reducing track width (TW) of magnetic read sensor to gain areal density, SH is needed to scale down to keep aspect ratio (TW/SH) which is for maintain resistance and signal constant of read sensor. Normally, magnetic read sensor is characterized to obtain the performance by using quasi-static testing (QST). QST is used to get the response of magnetic read sensor in applied external magnetic field by sweeping from negative to positive field without flying head over the media, and then the transfer curve and noise of magnetic recording are obtained. This tool is used for explain the whole performance of magnetic read sensor and indicate the optimized SH. However, QST information is not enough to characterize the behavior of magnetic read sensor by layer-level state.

To extend the study, this paper is proposed to further characterize the magnetic read sensor with various SH by using ferro magnetic resonance analyzer (FMRA) [1]. FMRA is equipment to analyze thermal magnetic noise that is related to magnetization fluctuation in different layer of read head sensor. FMRA is able to provide the explanation of reader sensor behavior by layer-level state in term of stiffness field which is related to efficiency of magnetic read sensor [6]. This paper is focused on analysis of the free layer behavior with various SH of TMR head by using FMRA without applying external field. Therefore, we can understand magnetic read head behavior and apply to enhance its detection capabilities for magnetic recording industry.

Principles and Theories

Magnetic read sensor is composed of multiple magnetic thin films which major components are free layer, pinned/reference layer, spacer and permanent magnet. This paper is focused on magnetization fluctuation of free layer that strongly affects to read ability. Ideally, magnetization orientation of free layer is aligned perpendicular to pinned layer to obtain the best sensitivity and symmetry sensor response of magnetic read sensor [1]. Nevertheless, the magnetization tilt is possible to occur as decreasing the dimension of magnetic read sensor to support areal density affects sensitivity and instability problem. The previous study is reported that thermal magnetic noise [4] is inversely proportional to dimension of magnetic read sensor and causes significant degradation of signal to noise ratio (SNR) [2]. Thermal magnetic noise is related to the motion of free layer and pinned layer magnetization which is performed by ferro magnetic resonance (FMR). This thermal magnetic noise can be studied theoretically by using the Landau-Lifshitz-Gilbert (LLG) equation [2], as shown in Eq.1, which describes the motion of a magnetization vector $\vec{M}$ in the presence of effective stiffness field $\vec{H}_{eff}$

$$\frac{d\vec{M}}{dt} = -\gamma\vec{M} \times \vec{H}_{eff} + \frac{\alpha}{M_s}\vec{M} \times \frac{d\vec{M}}{dt} \tag{1}$$

Here, γ is the gyromagnetic constant $\left(\gamma \approx 2.2\times10^5\ m/As\right)$, α is the Gillbert damping constant of the free layer and M_s is saturation magnetization. The effective stiffness field is calculated by Eq. 2

$$H_{eff,\phi} = H_{K,T}\cos 2\phi_0 + H_x \cos\phi_0 + H_y \sin\phi_0 \tag{2}$$

$H_{K,T}$ is the total anisotropy field resulted from crystalline and shape anisotropy terms by Eq. 3. H_x is longitudinal field direction due to permanent magnet hard bias. H_y is transverse field direction, which is perpendicular to free layer, due to external field. ϕ_0 is the angle between actual magnetization and ideal magnetization of free layer. When the magnetization of free layer is perpendicular to pinned/reference layer, $\phi_0 = 0$,

$$H_{K,T} = \frac{2K_u}{\mu_0 M_s} + \left(N_y - N_x\right)M_s \tag{3}$$

K_u is crystalline anisotropy energy, μ_0 is permeability of free space, N_x and N_y are the effective demagnetization factor in the x (parallel track width) and y (stripe height) direction, respectively. The magnetization fluctuation is studied by FMR spectrum which key parameters are frequency, amplitude and width at half maximum peak. The FMR frequency is determined by Eq. 4,

$$f_0 = \frac{\gamma}{2\pi}\sqrt{M_s H_{eff}} \tag{4}$$

FMR peak amplitude can be achieved from Eq. 5

$$V_p = I\Delta R\cos\phi\sqrt{\frac{k_B T}{\alpha\mu_0\gamma M_s H_{eff} V\left(H_{eff} + M_s\right)}} \tag{5}$$

The FMR full width at half maximum of spectra peak (FMR width at 50% of the peak amplitude) is determined by the following equation,

$$\Delta f = \frac{\gamma}{2\pi}\alpha M_s \tag{6}$$

Experimental method

The measurements are performed on TMR heads with the same track width but different SH target (-20nm, -10nm, -5nm, nominal, +5nm, +10nm, +20nm) in bar level. FMRA is equipped with high frequency probe (0.3-10 GHz) [1] and the external magnetic field is generated by quadrupole electromagnet. However, this paper is focused on free layer behavior of magnetic read sensor; as results the FMRA is carried on without applying the external magnetic field. FMRA and QST are performed on the same sliders with 140mV, voltage bias. FMR parameters are analyzed by FMR amplitude and frequency parameters that are able to describe the characteristic of free layer magnetization of magnetic read sensor. QST parameters are used to identify the whole performance of magnetic read sensor by Amplitude, SNR and Magneto-Resistive Resistance (MRR).

Results

This experiment is studied on FMR spectrum of TMR read head in the GHz range. Fig. 1 is shown the examples of FMR spectrum of a shortest (-20nm SH from nominal) and a longest SH (+20nm SH from nominal). For the shortest SH, FMR amplitude is 1.1 nV and FMR frequency is 8.1 GHz as shown in Fig. 1(a). While the longest SH, FMR amplitude is increased to 8.3 nV and FMR frequency is shifted to 4.8 GHz as shown in Fig. 1(b). The shorter SH of magnetic read sensor exhibits lower FMR amplitude with higher FMR frequency than the longer one.

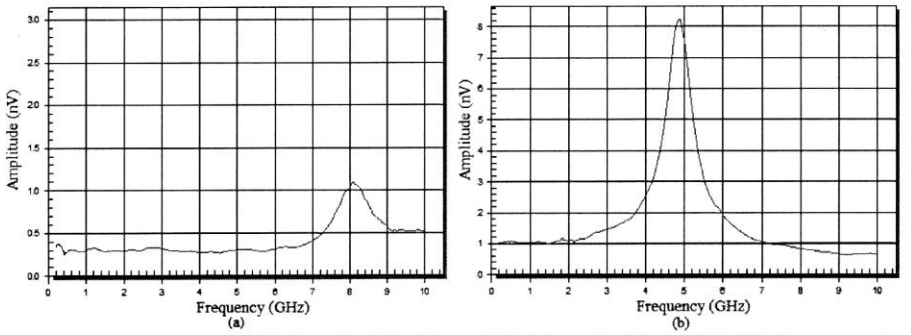

Fig. 1 FMR spectra on TMR head with -20nm SH (a) and +20nm SH (b) from nominal.

Fig. 2 (a) and (b) show FMR amplitude and frequency trend on TMR head with various SH targets. As shorter SH, FMR amplitude tends to decrease while FMR frequency leans to increase. QST result shows that Amplitude and SNR have decreasing trend with shorter SH as shown in Fig. 3(a) and Fig. 3(b), respectively. While MRR is increasing trend at shorter SH due to reduced resistance area. It is found that at shorter SH the effective stiffness field on free layer is increased which is analyzed from increasing FMR frequency as shown in Eq. 4 and decreasing FMR amplitude as shown in Eq. 5. QST result corresponds to the stiffness field trend that has less sensitivity and SNR with shorter SH. The experiments show that the fluctuation of stiffness field in free layer with various SH resulted from changed shape anisotropy as shown in Eq. 2 and Eq. 3.

In addition, this paper shows that the shortest SH gives 8 mV Amplitude which is not preferable in term of read ability. Therefore, it is necessary to study for SH optimization when the production has new reader design with reduced track width to support areal density in order to maintain the resistance and signal.

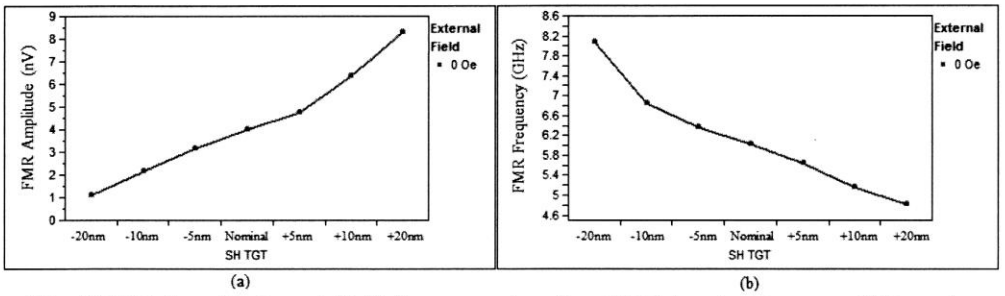

Fig. 2 FMR Amplitude and FMR frequency trend on TMR head with seven SH targets.

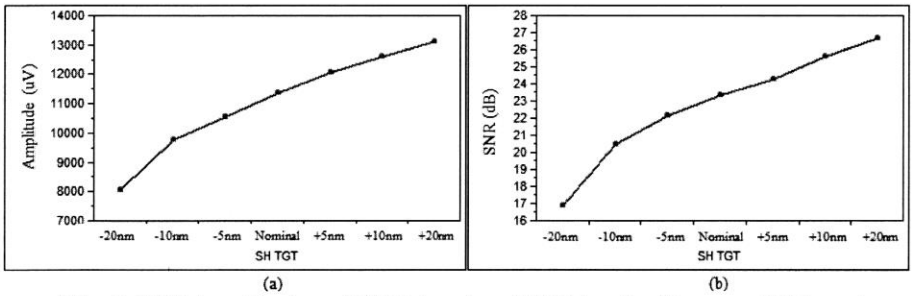

Fig. 3 QST Amplitude and SNR trend on TMR head with seven SH targets.

Conclusions and suggestions

Free layer behavior depends on SH scale. The SH is a correlated function of the effective stiffness field of free layer. It is referred to shape anisotropy which has an effect to read ability of magnetic read sensor. Base on reported result, the lowest FMR amplitude and the highest FMR frequency are found at the shortest SH which is originated from highest effective stiffness field of free layer. Therefore, magnetic read sensor shows least sensitivity with shortest SH. It is very important to study the characteristic of free layer in order to obtain optimized SH target for the yield of production and the read ability. However, the performance of magnetic read sensor is sensitive to the other components such as pinned/reference layer and permanent magnet that are characterized by FMR to study layer-level state with applying external magnetic field [3]. It is necessary to utilize FMR measurement combination with QST to analyze the behaviors of magnetic read sensor in order to understand the characteristic and extend the detection capability of magnetic recording industry.

References

[1] A. Taratorin, Measurement of effective free layer magnetization orientation of TMR sensors, IEEE Trans. Magn. Vol. 45, pp3449-3452, (2009)

[2] J. Jury, Student member, K. Klaassen, Jack C. L. van Peppen, S. Wang, Measurement and analysis of noise sources in giant magnetoresistive sensors up to 6 GHz, IEEE Trans. Magn. Vol. 38, pp3545-3555, (2002)

[3] G. C. Han, Y. K. Zheng, Z. Y. Liu and B.Liu, Field dependence of high frequency magnetic noise in tunneling magneto resistive heads, Journal of applied physical 100, pp063912-063916, (2006)

[4] O. Heinonen, H. S. Cho, Thermal magnetic noise in tunneling readers, IEEE Trans. Magn. Vol. 40, pp. 2227-2232, (2004)

[5] S. Kamwan, W. Pifitrojana and C. Sa-ngiamsak, Effect of track width and stripe height ratio on the characteristics of CPP-GMR and TMR heads, (2011)

[6] S.Wonglam and C. Sa-ngiamsak, Thermal and external magnetic field effects on ferromagnetic resonance characteristic of TMR heads, KKU journal, (2012)

Appendix B
Author biography

AUTHOR BIOGRAPHY

Name	Prapinporn Weawhongse
Date of Birth	Dec 22, 1983
Place of Birth	Phichit province
Address	97/49 Moo 9 Soi 2 Bangkhen Muang District Nonthaburi 11000
Bachelor Degree	Bachelor's degree of Electrical Engineer
Subject	Electrical Engineering
Institute	Department of Electrical Engineering, Faculty of Electrical Engineering Thammasat University
Year of Graduation	2006
Work Experience	Western Digital (2006-2015)
Department	Product Engineering